11th International Conference on Light and Color in Nature

University of Alaska – Fairbanks
Fairbanks, Alaska
5-8 August 2013

Chair: Dr. Ken Sassen

Abstracts

(2013 Alaska meeting group photo by Joseph A. Shaw)

Monday, 5 August

Session 1: Introduction, 0900-1030, Kenneth Sassen Chair

Welcome by Robert McCoy, Director of the Geophysical Institute

Opening Remarks by Kenneth Sassen, Committee Chair

0930 Invited: Atmospheric optics at the early Geophysical Institute, Glenn Shaw

1000 Keynote: Noctilucent clouds – ice clouds at the edge of space in the polar summer, Richard Collins

Session 2: Historical Optics, 1100-1200, Joseph Shaw Chair

1100: 2.1 The 1665 orange halo of Huygens's father - Gunther Konnen

1120: 2.2 The 35 minute green flash observed at Little America on 16 Oct 1929: a retrospective study - James Lock

1140: 2.3 The Nuremburg halo display of April 19, 1630 - Eva Seidenfaden

1300 Invited: Cloud Forms - Stanley Gedzelman

Session 3: Scattering Interference Phenomena, 1330-1430, Stan Gedzelman Chair

1330: 3.1 Revisiting the corona - Philip Laven

1400: 3.2 The heiligenschein - John Adam and Philip Laven

Session 4: Ocean Color/Optics, 1500- 1640, Philip Laven Chair

1500: 4.1 Colors of thermal pools in Yellowstone National Park - Paul Nugent, Joseph Shaw and Michael Vollmer

1520: 4.2 Caustics due to complex water menisci - Charles Adler and James Lock

1540: 4.3 Improvement of remotely sensed Kd (PAR) of shallow turbid water in the Yellow Sea - Bumjun Kil and Stephan Howden

1730-1900 Public Optics Demonstration, Kenneth Sassen Chair

Halomator and spectrodrom – a basement laboratory of atmospheric optics, by Michael Grossmann, Alexander Haussmann, and Elmar Schmidt

1930-2100 Conference Reception at the Museum of the North (light dinner)

Tuesday, 6 August

Session 5: Ice Crystal Halos/Arcs, 0900-1030, Michael Vollmer Chair

0900: 5.1 Invited: "Lowitz Arcs Revisited" - Robert Greenler, Les Cowley, and Robert Gorkin

0930: 5.2 Halos due to scattering by randomly oriented crystals - Gunther Konnen

0950: 5.3 Brightness profile of the 22 degree halo - Dave Lynch

1010: 5.4 Pyramidal halo phenomenon in Virginia June 21st, 2010 - Elmar Schmidt, T. Alan Clark, A. Haussmann, and Claudia Hinz

Session 5 continued: Ice Crystal Halos/Arcs, 1100 -1200, Michael Vollmer Chair

1100: 5.5 Streetlight halos - Walter Tape

1120: 5.6 Parry's arc from nearby light sources in Deadhorse, Alaska - Kenneth Sassen and Colin Triplett

1140: 5.7 Halo simulation progress report - Stanley Gedzelman

Session 5 continued: Ice Crystal Halos/Arcs, 1300-1350, Michael Vollmer Chair

1300: 5.8 Laboratory Demonstration, Position-related spectra within experimental parhelia: Simple hands-on experiments explaining the perceived color of sun dogs - K.-P. Mollmann and M. Vollmer

1330: 5.9 Brilliant colors from a white snow cover - Michael Vollmer and Joseph Shaw

Session 6: General Observations, 1350-1430, Gunther Konnen Chair

1350: 6.1 Unusual optical phenomena from mountain sites - Claudia Hinz

1410: 6.2 Establishment of the global meteopark system - Lai Bixing

Session 7 Biological Colors: 1530-1640, Robert Greenler Chair

1500: 7.1 On the purpose of color for living beings: a new theory of color organization - Katia Deiana and Baingio Pinna

1520: 7.2 How can a fish hide in the open ocean? - Robert Greenler

1540: 7.3 Iridescent colors in spider webs - H. Joachim Schlichting

1600: 7.4 Structural color of the butterfly wing scale - S. Yoshioka

1620: 7.5 Total internal reflection as solar protection for the Saharan desert ant Cataglyphis bombycina - Priscilla Simonis and Jean Pol Vigneron

Session 8 Mirages: 1640-1700, Robert Greenler Chair

1640: 8.1 Visible and invisible mirages: comparing inferior mirages in the visible and thermal infrared spectral range - Michael Vollmer, Joseph Shaw, Paul Nugent

Riverboat Discovery Chena River Excursion and Dinner, 1900-2200

Wednesday, 7 August

Session 9: Rainbows: 0900-1030, Walter Tape Chair

0900: 9.1 Invited: The natural tertiary rainbow- A photographic first - M. Grossmann

0930: 9.2 Photographic observation of a natural fifth-order rainbow - Harald Edens

0950: 9.3 Polarization and visibility of higher order rainbows - Gunther Konnen

1010: 9.4 Recent rainbow revelations - Robert Greenler

Session 9 continued: Rainbows, 1100-1200, Walter Tape Chair

1100: 9.5 New insights into the rainbow, Part 1 - Jean Louis Ricard, Peter Adams, and Jean Barckicke

1120: 9.6 New insights into the rainbow, Part 2 - Jean Louis Ricard, Peter Adams, and Jean Barckicke

1140: 9.7 Observation, photogrammetry, and analysis of a twinned rainbow - Alexander Haussmann

Session 9 continued: Rainbows, 1300-1430, David Lynch Chair

1300: 9.8 A physically based rainbow simulator taking the background into consideration - Moon R. Jung

1320: 9.9 Influence of non-spherical raindrop shapes on higher order rainbows - Alexander Haussmann

1340: 9.10 Flashes of light below the dripping faucet: an optical signal from capillary oscillations of water drops - Thomas Timusk

1400: 9.11 Digital Imagery Forum, A post-Faustian review of digital imagery: the good, the bad, and the weird - Dave Lynch, Leader

Session 10: Atmospheric Color and Polarization, 1500-1720, Raymond Lee Chair

1500: 10.1 Seeing, adapting to, and reproducing the appearance of nature - Mark Fairchild

1520: 10.2 What is the spectrum of skylight polarization? - Joseph Shaw and Nathan Pust

1540: 10.3 Measuring haze's effects on the colors and visible-wavelength spectra of clear skies - Raymond Lee

1600: 10.4 Views affected by a wavy air-water surface - Yoav Y. Schechner

1620: 10.5 Simulating dark sunlit clouds - Stanley Gedzelman

1640: 10.6 Shadows - Dave Lynch

The Light & Color Official Slide Show ("pretty picture session"), 1715 to whenever

Thursday, 8 August

Session 11: Astronomical Optics, 0900-1030, Charles Adler Chair

0900: 11.1 Invited: Twilight's Belt of Venus - Raymond Lee

0930: 11.2 Visibility of Sirius in broad daylight - Gunther Konnen and Piet Stammes

0950: 11.3 Some elementary but surprising facts about the sun's location in the sky - A. James Mallmann and Steven P. Mayer

1010: 11.4 Earthshine brightness and visibility - David Lynch

Session 11 continued: Astronomical Optics, 1100-1200, Kenneth Sassen Chair

1100: 11.5 The use of light and color in astrophysical imaging - Travis A. Rector, Zoltan Levay, Lisa Frattare, Jayanne Englllish, and Kirk Pu-uohau-Pummill

1120: 11.6 Lunar eclipse photometry across the world – first correlations - Elmar Schmidt

1140: 11.7 Using light and color to detect life on Earth-like extra-solar planets - Eyal Schwartz, Stephen G. Lipson, and Erez N. Ribak

Concluding Remarks and Challenge - Kenneth Sassen

Afternoon Tour of Chatanika gold mining area (lunch) and UAF Poker Flat Rocket Range

(Invited talk)

Atmospheric optics at the early Geophysical Institute

Dr. Glenn E. Shaw – glennshaw@alaska.net

Geophysical institute and Atmospheric Sciences Program, University of Alaska Fairbanks, Fairbanks. Alaska, USA.

The polar zones contain unusual and interesting displays of visual optical displays. It is only natural therefore that a wide variety of investigations, mostly informal and unfunded, have taken place on atmospheric optics over the years. These include, especially investigations of mirages, formed by light passing through the complex thermoclines in the polar atmosphere, but also investigations of the wide variety of sky arcs formed by light refracting through ice crystals. Of especial importance and quite famous is the theoretical and observational work of Walter Tape at the UAF Mathematics Department. In addition work has been carried out in probing the dust structure of the stratosphere and upper atmosphere using multiwavelength twilight photometry, and polarization of the sky was investigated during conditions of total solar eclipse. There are often prolonged and spectacular displays of the green flash as the sun slides along the horizon in the winter months; the author authored a theoretical paper on this subject in 1976. Finally some theoretical work has been carried out attempting to deduce the temperature structure within the lower troposphere by inverting mirage images. Finally, cans of the sky radiance along with precision multiwavelength measurements of atmospheric extinction have been used to deduce the size distribution of suspended atmospheric aerosols.

(Invited keynote talk)

Noctilucent clouds – ice clouds at the edge of space in the polar summer

Dr. Richard L. Collins

Geophysical institute and Atmospheric Sciences Program, University of Alaska Fairbanks, Fairbanks. Alaska, USA

In this talk we review the science and optics of Noctilucent clouds (NLCs). NLCs also called Polar Mesospheric Clouds (PMCs) are the highest clouds on Earth. These clouds form in the summer near 80 km in the polar regions where the atmosphere is colder in summer than winter. These clouds have been studied since the late 1800's and were one of the first indicators that the atmosphere extended to such heights. More recently they have attracted attention as an indicator of global change. This talk presents contemporay satellite and ground-based observations of these clouds. The talk also highlights laser radar (or lidar) observations that have been made in Alaska by faculty and students at the University of Alaska Fairbanks.

The 1665 Orange halo of Huygens's father

Gunther Können

During the ceremony of restoration of the Principality Orange (near Avignon, France) in 1665, led by Christiaan's father Constantijn Huygens, a 'solar crown' appeared in the sky, apparently a divine sign of approval. A nearly forgotten contemporary color engraving of this miraculous event has survived. Constantijn seized the opportunity by using to his advance the general euphoria among the citizens caused by the appearance. I believe that Constantijn exactly knew what was going on in the sky because of his son's work on halo theory. Given its brightness and its time of appearance, it seems plausible that the most prominent halo in the Orange halo display was a circumscribed halo rather than the circular 22° halo, as has probably during ages been the case for the majority of other high-sun halos causing general commotion, starting with the Octavian halo (44 BC) and lasting via the Chernobyl halo (1986) till bright high-sun halos appearing in our days.

Initially the picture of the Orange halo was immensely popular, but become readily forgotten when the 'omen of good fortune' failed to materialize and Orange was captured by Catholic France. Fortunately a beautiful color picture survived.

The 35 minute green flash observed at Little America on 16 Oct 1929: A retrospective study

James A. Lock

Physics Dept., Cleveland State University, Cleveland OH 44115

Abstract: On 16 Oct 1929 five members of the Byrd Antarctic Expedition observed an intermittent green flash for 35 minutes at the Little America station as the sun slowly set over the Southern horizon. The flash was almost certainly associated with a mock mirage, which is known to occasionally produce somewhat longer than average flashes at temperate latitudes. Assuming all the atmospheric conditions required for the existence of a green flash are met for the entire observation period, I address the constraints imposed on the time duration of a green flash in the Arctic or Antarctic regions due to the orbital dynamics of the earth-sun system.

The Nuremburg Halo Display of April 19, 1630

Eva Seidenfaden eva.seidenfaden@t-online.de

Nikolaus-Mommer-Str. 78, 54296 Trier, Germany

On April 19, 1630, the town of Nuremburg witnessed a complex halo display that inspired both engravers and scholars. With three different single prints and a pamphlet comprising 24 pages, it belongs to best-documented 17th century halo displays. Furthermore, one of the engravings clearly shows a Wegener arc, rarely depicted in ancient halo literature.

The different published documents both reveal a great public interest in celestial phenomena, a state of knowledge largely influenced by the classic Latin and Greek tradition and diverging religious implications. They reflect the will to harmonize the conflict between religious beliefs and science as we understand it today, making them a valuable source for the history of science. We try to analyze the illustrations and, above all, the texts, comparing them to a pamphlet written by Erasmus Francisci on atmospheric phenomena and a selection of other 17th century sources.

(Invited talk)

Cloud Forms

Stanley David Gedzelman

This lecture on how clouds get their forms is illustrated with photographs, paintings, simulations, and time lapse photography. The lecture includes a brief history of cloud paintings because artists identified virtually all the cloud forms centuries before Luke Howard and Jean Baptiste de Monet Lamarck first named and classified clouds scientifically in 1802-1803. Howard's genera include cirrus (trails of falling ice crystals twisted by the winds), cumulus (blobs of rising buoyant air), stratus (cooling or obliquely rising layers of air) and variants thereon.

All clouds are produced by cooling air below the original dew point temperature. When this happens, spherical droplets and/or hexagonal ice crystals that produce so many atmospheric optical phenomena form and grow.

Cooling processes include contact with a cold surface, loss of heat by radiation, and rising motions. By far the fastest way to cool air is to make the air rise. For this reason, most clouds and virtually all precipitation are produced by rising air.

Most droplets and crystals are so tiny they have little terminal velocity and are swept along with the air as it rises and sinks. As a result, most clouds represent the signature of the winds and their different forms reflect the different patterns of rising and sinking air. Ice crystals often grow large enough to have an appreciable terminal velocity but are still small enough so that they move with the wind. The patterns of the resulting cirrus fall streaks reflect the wind shear.

There are only a few basic cloud forms because there are only a small number of distinct patterns of air motions including waves, plumes, penetrative and cellular convection, wind shear, and vortices. Cloud forms also reflect the rate of cooling, whether the air motions are laminar or turbulent, and the vertical profile of humidity. Clouds that form in rapidly cooling air, such as growing cumulus tend to have a solid appearance with distinct edges, while clouds that form in slowly cooling air, such as fog tend to have indistinct or smoother edges. Turbulent convection produces highly corrugated cumulus while laminar wave motions produce the smooth edged altocumulus lenticularis, i. e., mountain wave clouds. Clouds can appear laminated when the atmosphere contains multiple alternating humid and dry air layers.

Finally, some attention is devoted to exploring the relation between cloud form and atmospheric optical phenomena. For example, because the scattering angles vary with droplet size, the most vivid coronas and glories are produced by laminar wave clouds because they tend to produce the smallest range of drop sizes in a given volume of cloudy air.

Revisiting the Corona

Philip Laven

The atmospheric corona, seen as colored rings around the sun or moon, is considered to be a well-understood phenomenon defined by the Fraunhofer diffraction formula:

$$I(\theta) \;\alpha\; \left(x^2\left[\frac{1 + \cos\theta}{2}\right]\left[\frac{J_1\,(x \sin\theta)}{x \sin\theta}\right]\right)^2$$

where ϑ is the scattering angle; J_1 is the first-order Bessel function; $x = 2\pi r/\lambda$; r is the radius of the scattering sphere and λ is the wavelength of the incident light. This equation gives results which are very similar to those calculated using Mie theory – at least for particles with $r > 6$ µm. However, Mie theory simulations for the scattering of sunlight by smaller particles (e.g. for 1 µm < r < 3 µm) show some puzzling behavior and strange colors, which are very sensitive to particle size and scattering angle – as shown below on the right side of Fig. 1. This sensitivity to particle size offers an explanation for the colors of iridescent and mother-of-pearl clouds, both of which display rapid color changes near the edges of clouds.

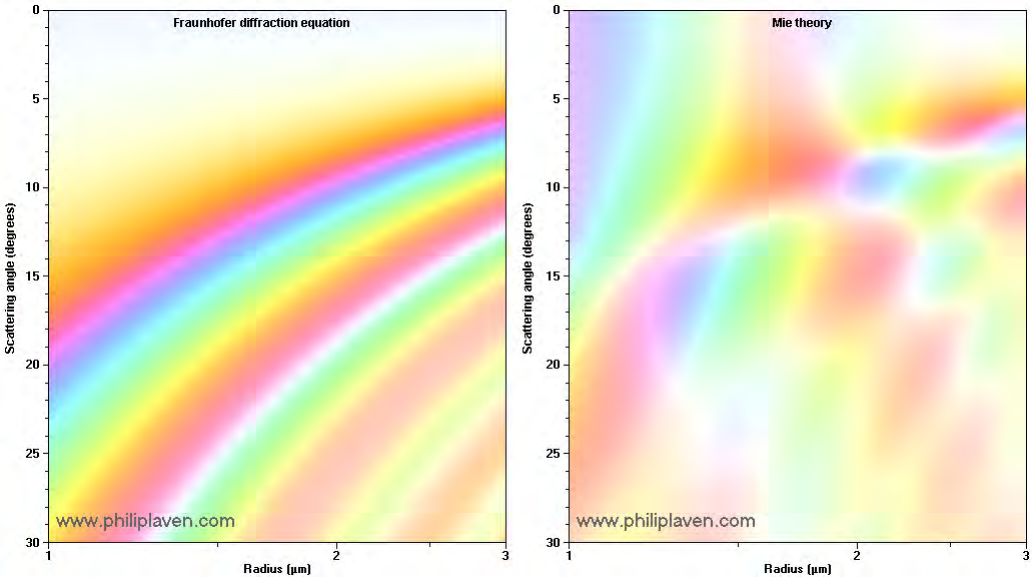

Fig. 1 Scattering of sunlight as a function of particle radius r and scattering angle ϑ calculated using the Fraunhofer equation (left) and Mie theory (right)
N.B. The above diagrams show only the saturated colors (not the intensity) of the scattered light.

Returning to the corona caused by larger particles, many authors have deduced the particle size from the angular size of the corona's rings – which correspond to maxima in the last term of the above equation. The first 4 maxima occur when $x \sin\vartheta = 5.136$, 8.418, 11.62 and 14.796 – corresponding to $\sin\vartheta = 0.8174\lambda/r$, $1.3398\lambda/r$, $1.8494\lambda/r$ and $2.3549\lambda/r$. If ϑ is measured in degrees and r is measured in µm, the 4 inner rings of the corona for red light ($\lambda = 0.65$ µm) should therefore appear at $\vartheta = 30.5/r$, $50/r$, $69/r$ and $88/r$.

The above calculations assume monochromatic illumination, but simulations of coronas caused by scattering of sunlight show red rings at $\vartheta \approx 16/r$, $31/r$ and $47/r$. The red ring at $\vartheta \approx 16/r$ is a complete surprise, but the next two rings occur at values of ϑ close to those predicted for monochromatic light. The additional ring at $\vartheta \approx 16/r$ can be easily explained, but anybody using the Fraunhofer formula to determine the size of the particles causing the corona would overestimate the particle size by a factor of 30.5/16 ≈ 2. Several published papers seem to have made this error – including one under my name!

The Heiligenschein

John Adam & Philip Laven

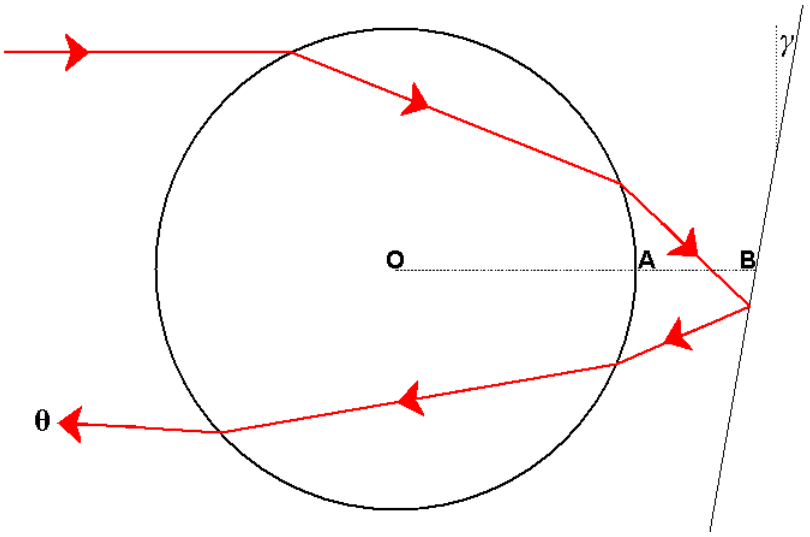

The Heiligenschein is generally considered to be caused by the scattering of light from spherical dew drops "sitting" on small hairs on blades of grass. As shown by the sample ray path in the above diagram, incident rays can pass through the dew drop, be reflected by the blade of grass and then be re-transmitted through the dew drop.

As we are not aware of any quantitative calculations supporting this theory of Heiligenschein, we have used geometrical optics to calculate the intensity of the scattered light as a function of the scattering angle ϑ (taking account of the radius OA of the dew drop, distance AB between the drop and the blade of grass, and the tilt γ of the blade of grass). The results show that the focussing of rays near the reflecting surface produces very sharp enhancements in the scattered intensity at specific values of ϑ.

The presentation will compare images of the natural Heiligenschein with computer simulations derived from our calculations, supplemented by images of experiments using large glass spheres.

Colors of Thermal Pools in Yellowstone National Park

Paul W. Nugent and Joseph A. Shaw, Montana State University, Bozeman, Montana, USA (jshaw@montana.edu)
Michael Vollmer, Brandenburg University of Applied Sciences, Germany

Abstract

The thermal pools in Yellowstone National Park are world-famous for their variety of colors and geyser activity. Some of the color variation is caused by different types of bacteria that live in these boiling waters, but much of the visual color also results from scattering and absorption in the water. To build simple models to help understand these patterns, we visited Yellowstone Park during August 2012 and made a variety of measurements in different regions of several pools. At each location we recorded visible and near-infrared spectra, visible images, and thermal infrared images in the 8-14 μm wavelength range. These data show that the hottest pools are devoid of bacterial life, and exhibit colors with a smooth gradation from grayish-white at the outer edge to deep blue at the center where the pool is deepest. Conversely, the cooler pools contain bacterial mats that appear yellowish-orange or green in color, and these pools exhibit colors that fade to green and eventually black at their deepest points. In this presentation we will show measurements and model results for several Yellowstone thermal pools.

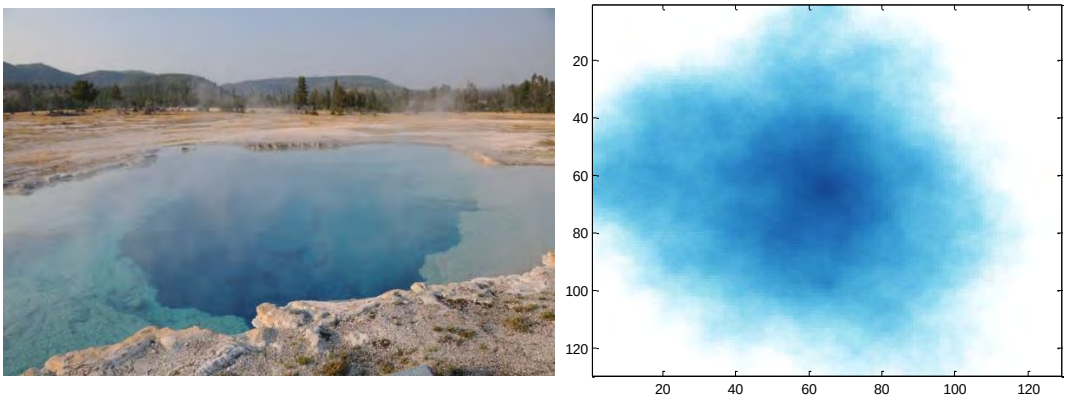

Figure 1. Sapphire Pool photograph (left) and simulation (right) – the hottest measured pool.

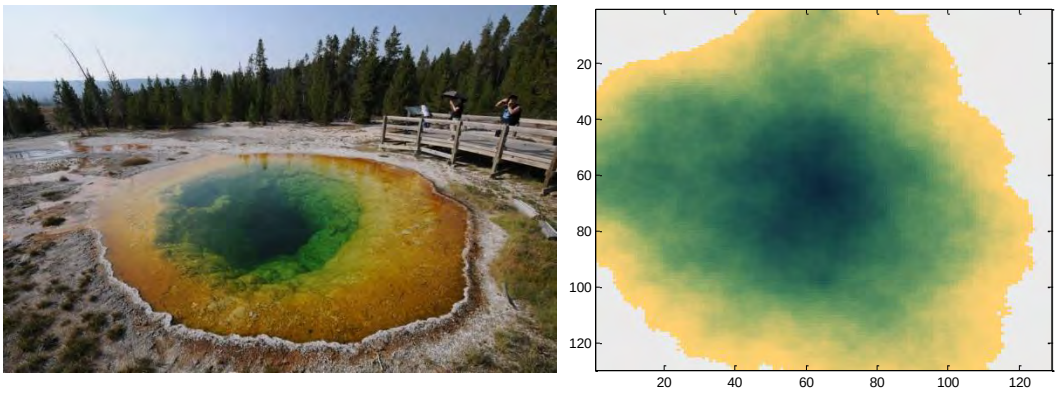

Figure 2. Morning Glory Pool photograph (left) and simulation (right) – a cooler pool.

Caustics due to complex water menisci

Dr. Charles L. Adler* and Dr. James A. Lock†

*Physics Department, St. Mary's College of Maryland, St. Mary's City, MD 20686

†Physics Department, Cleveland State University, Cleveland, OH 44115

The shadows of objects either floating or immersed in water like leaves or a boat's rope are complicated due to the refraction of light by menisci at the boundarys where they enter the water. Despite the typically minute size of the meniscus, the effect on the shadow can be profound. One well-known phenomenon is the "shadow-sausage" caustic due to a raised meniscus, which creates a "break" in the shadow, appearing as a band of light at the portion of the shadow corresponding to the line where the object enters the water.[1]

Berry and Hajnal examined caustics produced by menisci due to a straight edge and a sphere. [2] In each case the caustics were due to a meniscus depressed below the surface of the water due to the weight of the floating object. However, other types exist, such as the shadow-sausage caustic mentioned above where the effect is due to a raised meniscus clinging to a cylindrical object immersed in the water. Others may have complicated boundaries where in one section the meniscus is depressed and another raised; this is commonly seen in photographs of leaves floating in a shallow pool illuminated from above.

We examine the optics of such complex menisci both experimentally and theoretically. In particular, we look at a surface where roughly half of the boundary consists of a meniscus raised above the water surface while the other half is depressed below it. Such a system can be experimentally realized by floating an eccentrically weighted circular coin or token. We also examine complications due to multiple floating objects.

1. "Analysis of the shadow-sausage effect caustic", James A. Lock, Charles L. Adler Jonathon Mulholland, Brian Keating and Diana Ekelman, *Applied Optics,* **42** (2003) 418-428

2. "The shadows of floating objects and dissipating vortices", M. V. Berry and J. V. Hajnal, *Optica Acta,* **30** (1983) 23-40

Improvement of remotely sensed Kd (PAR) of shallow turbid water in the Yellow Sea

Bumjun Kil*[1] and Stephan Howden[2]
[1] Doctoral student
[2] Associate Professor

Department of Marine Science in University of Southern Mississippi, Stennis Space Center, MS

The remotely sensed diffuse attenuation coefficient at photosynthetic available radiation (Kd (PAR)) in the Yellow Sea was compared with estimated values from Secchi depth (SD) to investigate the effect of turbid condition to the satellite based optical coefficient. As a result, the difference between Kd (PAR) from Aqua satellite and estimated values from SD which is collected by Korea Oceanographic Data Center (KODC) was increased as shallower the bottom depth. Especially, the difference presented larger in winter season probably because vertical mixing by strong wind and sea surface cooling that elevates the resuspension of the suspended particle matter (SPM) related with bottom depth in shallow coastal region (Choi et al., 1998). Assuming that the resuspension of SPM is affected by shallow bottom depth, we attempted the modification of Kd (PAR) by adding the modeled difference of Kd (PAR) between Aqua satellite and SD to existing Kd (PAR) depending on bathymetric condition based on ETOPO1 from National Geophysical Data Center (NGDC). Consequently, the generated Kd (PAR) showed improved in shallow turbid area but the model for modifying existing coefficient should be applied in separate season due to strong mixing condition in winter.

(Invited public demonstration)

Halomator and Spektrodrom – A Basement Laboratory of Atmospheric Optics

Michael Grossmann, AK Meteoros, Kaempfelbach, Germany
Alexander Haussmann, Technical Univ. of Dresden, Germany
Elmar Schmidt, SRH Univ. of Applied Sciences, Heidelberg, Germany

The main author of this lecture is trained and employed as a professional toolmaker, so he advocates a hands-on approach to understanding atmospheric optics phenomena. Guided by the work of Greenler and Vollmer, the first experiments used hexagonal column crystals made from acrylic glass, to be rotated in a two-axis cradle. This set-up already showed the tangent and Parry arcs, the parhelic circle with sundogs, as well as the subsun and subparhelia. Still not satisfied with the results, the author miniaturized the cradle and made it rotating quite fast in three axes, one powered electrically and two by compressed air. By clamping the rolling axis, all the previous phenomena can be shown, but by allowing all rotary movements, the standard ring-halo is shown. Besides the differing refractive indices of acrylic and ice, the limitation presently resides in manufacturing imprecisions of the model crystals. The simulation of rainbows of many orders with hanging or standing water drops and laser light is straightforward, but often unrealistic due to deformation of the drops. Therefore, a modern version of Billet's experiments was designed, which uses a laminar cylindrical flow of water, and white light by just a few pixels of a video projector. It is surrounded by a circular projection screen. Using slightly skewed rays, which are therefore "climbing" up the cylindrical beam of water and exiting from it in proportion to the number of partial reflections, is able to produce a simultaneous display of the first six rainbow orders in white light.

LOWITZ ARCS REVISITED

Robert Greenler, Madison, Wisconsin
Les Cowley, Norfolk, England
Robert Gorkin, Dover, Delaware

Abstract

Tobias Lowitz published a sketch of a remarkable halo display that he observed in St. Petersburg in 1790. Two arcs shown on his drawing take the name Lowitz Arcs from this publication, but photographic evidence confirming the reality of these elusive arcs took more than two centuries to obtain. A computer simulation--published in 1979--suggested a mechanism for their appearance, and, eventually, in the 1990s and 2000s several photos were taken that verified their existence. Some of these photos also showed other components of the Lowitz-Arc display predicted by the computer simulation, but not reported in the original drawing. Recently some photographs--taken in 1988--have come to light that show well-developed arcs that are nicely simulated by light going through plate crystals that take all rotational positions about a horizontal axis as they fall through the air.

Halos due to scattering by randomly orientated crystals

Gunther Können

The radiance distribution of halos due to randomly oriented ice crystals differs greatly from the radiance distribution of halos due to preferentially oriented ice crystals. This difference is fundamental. A formalism is shown that is able to describe scattering of light by randomly oriented crystals and applied to 4 examples, among them the circular 22° halo and the antisolar halospot.

Brightness Profile of the 22 Degree halo

David K. Lynch

Thule Scientific

Abstract

The brightness profile of the 22 degree halo is highly variable from display to display. Sometimes it is thin, bright and colorful, other times it is broad, faint and colorless. In this paper we discuss the factors that influence the halo profile such as diffraction, particle shape, and ice porosity and temperature.

We suggest that a major cause of profile variation is deviations from the 60 degree prism angle, caused in part by sublimation of surface ice which is strongest where two adjacent prismatic faces meet. Sublimation increases the prism angle in some parts of the crystal, decreases it in other parts, thereby smearing out the halo.

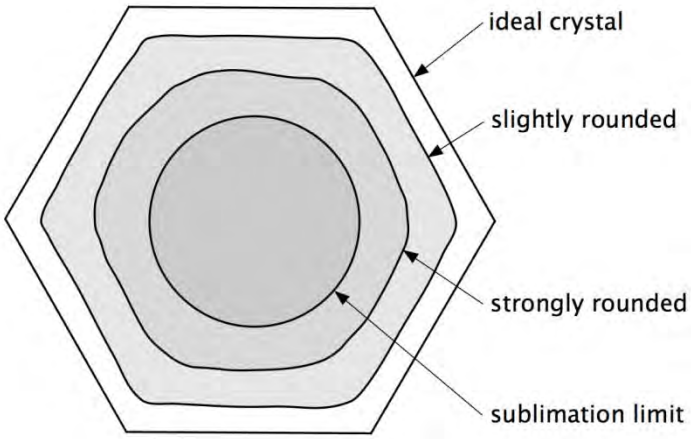

With a distribution of ice crystal sizes and extent of sublimation, the resulting range of prism angles produces a broader, fainter and less colorful halo. In the limit of profound sublimation, the ice's cross section becomes nearly circular, and the "halo" fades away leaving only the forward scattering peak of Mie theory (aureole).

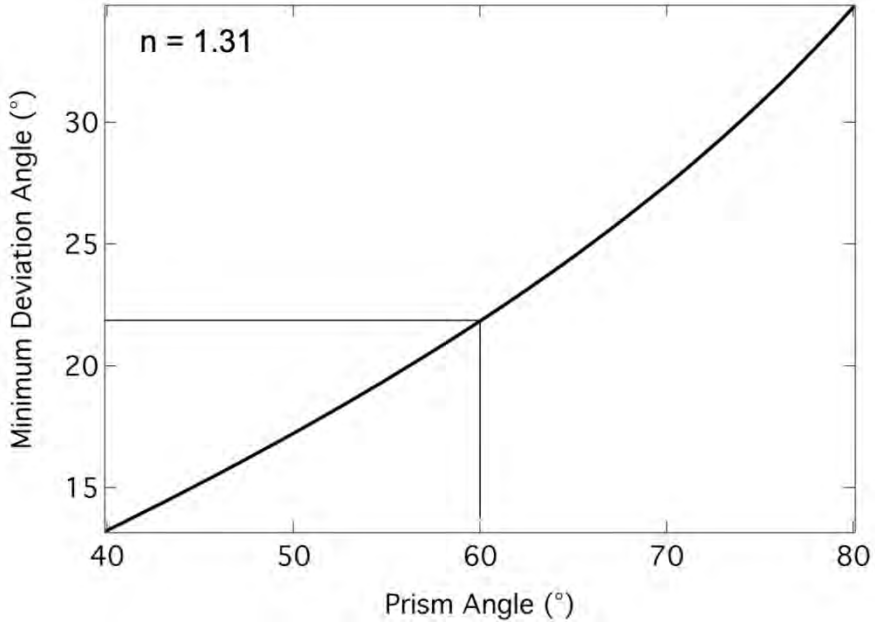

Pyramidal Halo Phenomenon in Virginia June 21st, 2010

Elmar Schmidt, SRH University of Applied Sciences, Heidelberg, Germany
T. Alan Clark, University of Calgary, Canada
A. Haussmann, Technical University, Dresden, Germany
Claudia Hinz, AK Meteoros, Schwarzenberg, Germany

Just two days, after the 10th Light & Color in Nature Conference in Maryland ended, a large scale front system approached the U.S. East Coast from the interior, allowing two of the authors, who still were traveling in the area to observe and photograph a rare odd ring halo display, comprising radii of, 9, 18, 20, 23/24 and 35 degrees. These are known to be caused by pyramidal ice crystals. In central Virginia the display lasted for at least two and a half hours during which the Sun's elevation angle decreased from 57 to 29 degrees. In the final hours, column arcs were also appearing.

Streetlight Halos

Walter Tape
University of Alaska–Fairbanks

A good streetlight halo display is nearly psychedelic, but streetlight halos are mind-altering from a scientific perspective as well. Streetlight halos make up a kind of higher dimensional halo world, with the familiar 'classical' halos occupying only a tiny niche of it. Once you enter that world, your notion of a halo will never be the same.

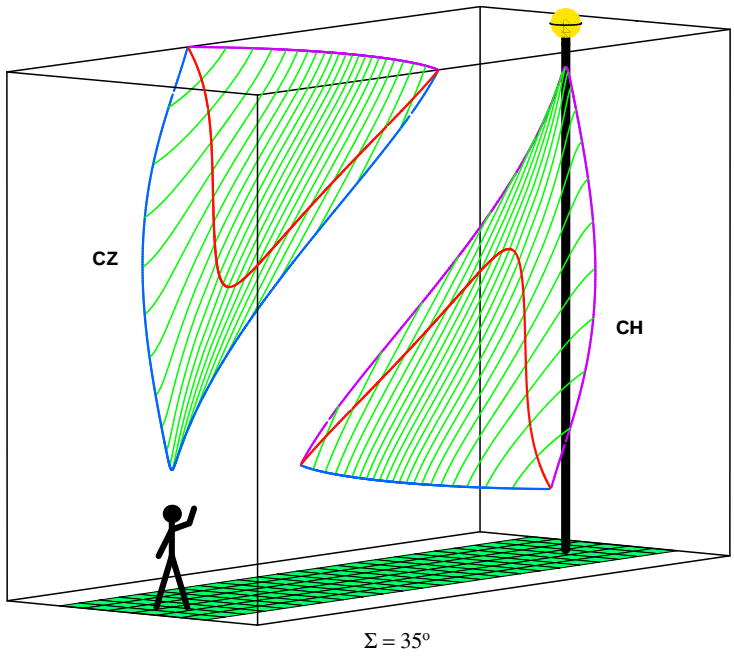

Streetlight circumzenith and circumhorizon arcs.

Folks who wish to cheat and do some homework can go to:

https://sites.google.com/a/alaska.edu/walt-tape/unpublished

Parry's Arc from Nearby Light Sources in Deadhorse, Alaska

Kenneth Sassen and Colin Triplett

Geophysical Institute, UAF

Fairbanks, Alaska, U.S.

ABSTRACT

During a light snowfall on the northern Alaskan coast an unusual optical display was photographed caused by local light sources at a temperature of ~-5°C. The images reveal unspectacular light pillars, which are topped by two narrowly separated "V"-shaped arcs starting 15 degrees above the horizon (see Figure 1). The most apparent explanation is a combination of Parry's and tangent arcs caused by singly- and doubly-oriented column crystals, which can also create artificial light pillars according to earlier ground-based observations. These arcs should overlap in the case of parallel light rays from the sun or moon at the horizon, but not in the case of divergent local light. We are currently modeling this situation using ray optics to ascertain the true cause of this display.

Figure 1.

Halo Simulation Progress Report

Stanley David Gedzelman

Abstract

At the 2010 meeting, I presented simulations of a multiple scattering Monte Carlo halo model in which a cloud layer is surrounded by clear, molecular air layers and a hazy atmospheric boundary layer. The model reproduced reasonable facsimiles of photographs of various halo displays but suffered from two main shortcomings, namely, 1: the simulations appeared spotty due to low dot density of background sky light and, 2: smoothing designed to reduce the spottiness spuriously broadened and smudged all halos.

I will report on the progress made since the 2010 meeting to rectify the abovementioned problems. The spurious broadening of the halos is eliminated by use of an algorithm that smoothes only the background skylight. Beams are classified as halo beams if they are scattered only once and only by a crystal. All other beams are classified as sky beams. Halo and sky beams of each of 61 wavelengths are filed separately into tiny bins (≈0.25° diameter). Only the field of bins for the sky beams is smoothed. Spottiness of the background skylight is reduced by improved smoothing routines. The smoothed sky beams are then conjoined with the halo beams to produce more nearly photographic simulations.

Position related spectra within experimental parhelia:
simple hands on experiments explaining the perceived color of sun dogs

Klaus-Peter Möllmann and Michael Vollmer, Brandenburg University of Applied Sciences, Germany,
moellmann@fh-brandenburg.de and vollmer@fh-brandenburg.de

Abstract:
Color in halos is due to refraction effects, however, with the exception of a few very brilliant colorful halos such as e.g. the circumhorizontal arc, many refraction halos only show colored edges. Examples are e.g. the 22° rings. Parhelia offer a slightly better color separation, however in most cases, only the red inner edge with adjacent yellow is pronounced whereas the color of the outer regions resembles more or less white due to the superposition of all colors contributing to the underlying minimum deviation effect.
The respective spectra and consequently the respective perceived color at each location within the parhelia can of course be computed theoretically. Here we complement such a theoretical analysis by an easy hands on and very colorful experimental visualization of the spectra as a function of deviation angle from the light source. The idea behind is to spectrally analyze experimental parhelia from a rotating prism by directing the refracted light through a second dispersive element orthogonal to the first prism (see Fig. 1). The experiment will be demonstrated and results, including simultaneously recorded spectra with a portable USB spectrometer, are discussed.

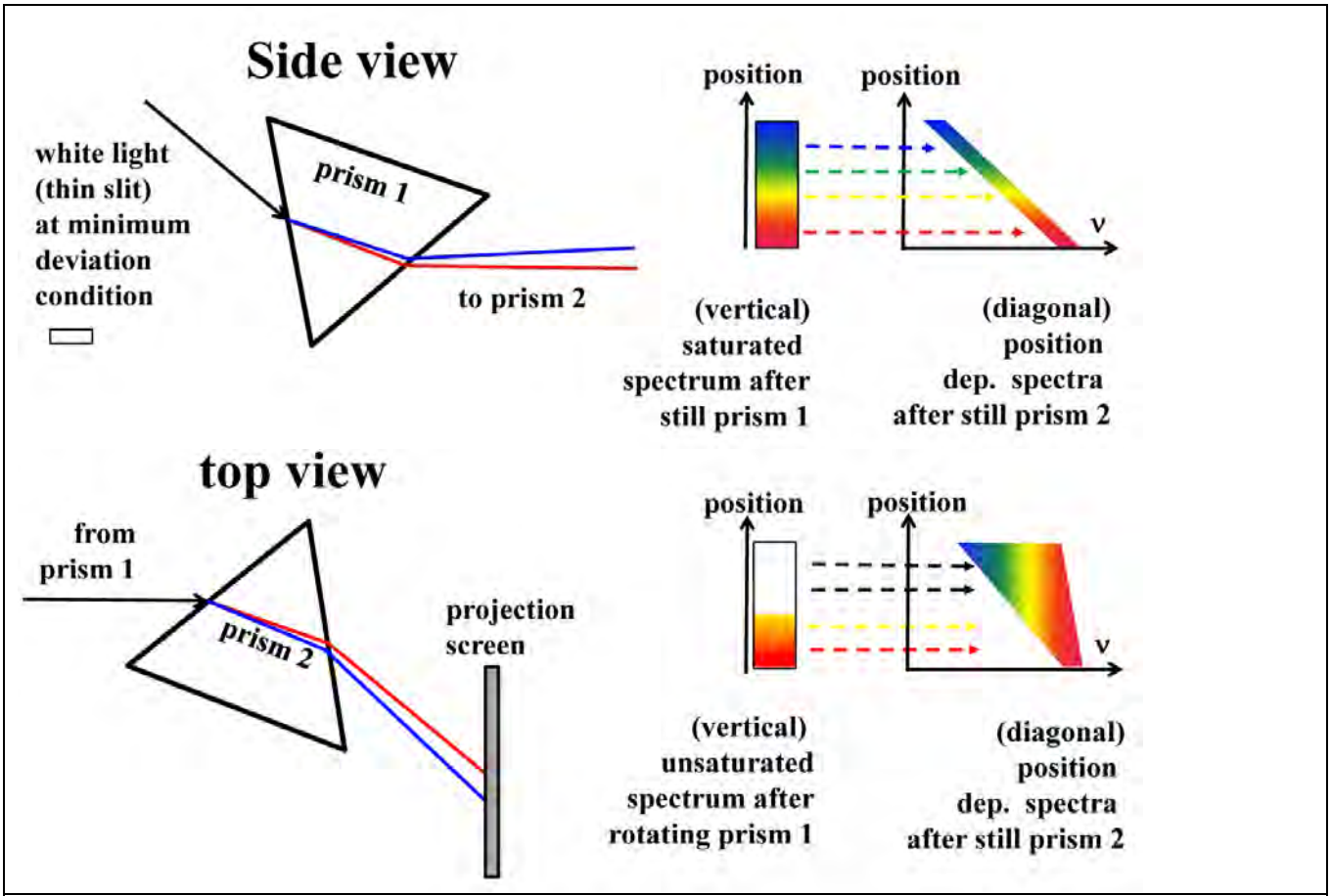

Fig. 1: Scheme of experimental set up to demonstrate the position related spectra within parhelia.

Brilliant colors from a white snow cover

Michael Vollmer, University of Applied Sciences Brandenburg/Germany vollmer@fh-brandenburg.de
Joseph A. Shaw, Montana State University, Bozeman/Montana

Abstract:
Surprisingly colorful views from sparkling white snow are possible [1,2], see Fig. 1. It is well known that similarly colorful features can exist in the sky whenever appropriate ice crystals are around. However, the transition of light scattering from snowflakes in the air to scattering from those in snow on the ground is not trivial. Photos and videos from brilliant colorful sparkles observed in white snow covers are presented and discussed also with respect to observation conditions such as morphology changes of snow upon meteorological changes and respective duration of the phenomena.


a


b

Fig. 1: Snow covered area showing colorful sparkles focused close to the ground (a) as well as focused closer to infinity (b).

References:

[1] D. K. Lynch, W. Livingston: *Color and Light in Nature*, 2 edn. (Cambridge Univ. Press, Cambridge 2001)
[2] M. Vollmer, J. Shaw, *Brilliant colors from a white snow cover*, Physics Education, in print

Unusual optical phenomena from mountain sites

Claudia Hinz, Oswaldtalstr. 9, 08340 Schwarzenberg, Germany

On high mountains one stays in the middle of the weather rather than on its bottom, which offers a quite different view on several optical phenomena. One example is that just before sunrise supersuns and superparhelia may become visible, as due to the lowering of the astronomical horizon the sun may be mirrored upwards by horizontally oriented crystal faces. When after sun rise the sun climbs higher in the sky and thus the subsun sinks more and more into the valleys, the chance increases that the subsun (or subparhelia) arises from different ice cloud layers - resulting in offset subsuns due to tildet ice plates. The appearance of fog bows and glories also vary with the observer's altitude on the mountain. If they appear in medium-high clouds, their interferences often become much more vivid, because the drop size in altocumulus clouds is consistently smaller and relatively monodisperse compared to the conditions in cumulus clouds. In addition to the phenomena mentioned above, this talk will also touch on and present pictures of various mountain-site oddities like irregular coronae, kinked rainbows (probably caused by strong shear winds), downward facing zero-order glows, deformed glories, subhorizon haloes and crepuscular rays reflected from the surfaces of lakes in the valleys.

Establishment of the Global Meteopark System

Lai Bixing [1, 2]

1 *Institute of Atmospheric Physics, Chinese Academy of Sciences, Beijing , 100029*

2 *Research Center of Landscape–Meteorology, Central-South University of Forestry & Technology, Changsha, 410004*

Email: lyrebs@163.com

Meteorological landscapes, such as rainbow, halo, corona, glory, aurora, sunrise, rosy clouds, sea of clouds, snow and glacier, wind and rain, are all bright and colorful. And their resources are very abundant. However, they have not been incorporated into any of the four systems defined by the UNESCO (National Park & Reserve Area System, the Natural and Cultural Heritage of the World, Man and Biosphere Program, Geopark Program)， which have long been dedicated to the professional earth heritages protection. In this article, we will bring up a new concept, "***Meteopark***"（that is a special rare natural area with the meaning of meteorology, higher value in aesthetics, a fairly in scale, a composed mainly of meteorological landscape, mix together other natural phenomena and humanity landscape）， discuss its functions, features, scopes, future developments, accomplish route chart and finally the establishment of Global Meteopark System. The aim is to assess the resources of meteorological landscape and to provide a platform for sustainable development and utilization of the resources in the world.

Keywords: Global, "Meteopark", System, Establishment, the Resources of Meteorological Landscape.
(There are several photos in the following pages)

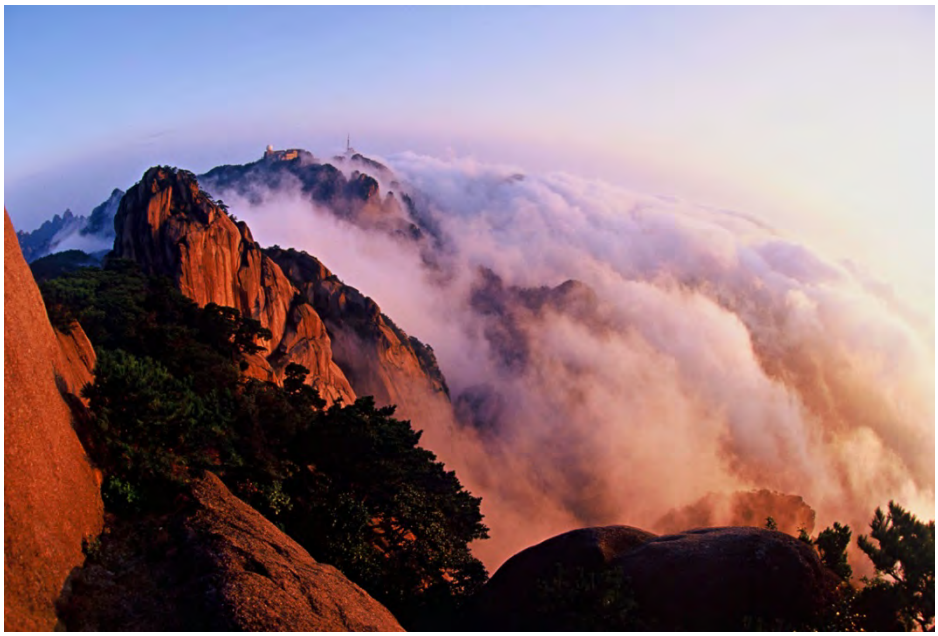

The sea of cloud flew on without stopping, Mt. Huang, China

The pines stand gracefully erect covering with rime，Mt Huangshan, China

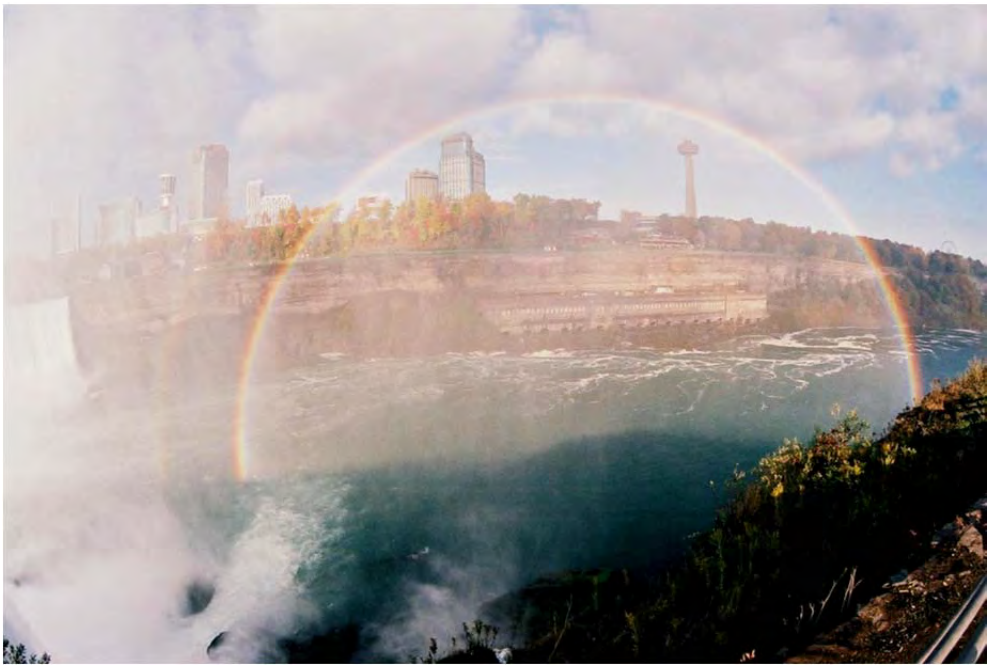

The colorful rainbow on Niagara Falls 2010-10-20

Glory on Mt. Huangshan, China 2004-8-27

Travelers did not know the glory had appeared in their vicinity.

Mt. Huangshan, China. 2004-8-27

Travelers were appreciating the glory (guided by the author)

on the Lotus of Mt. Huangshan, China 2010-7-17

(All the photos were taken by Lai Bixing)

On the purpose of color for living beings: A new theory of color organization

Katia Deiana and Baingio Pinna

Department of Architecture, Design and Planning
University of Sassari at Alghero, Alghero, Italy

Abstract:

Phylogenetic and paleontological evidence indicates that in the animal kingdom the ability to perceive colors evolved independently several times and has existed for at least half a billion years. This implies a high evolutionary neural investment and suggests that color vision has some fundamental and specialized functions providing biological advantages. What are these advantages? What is the purpose of color for living beings? Why are animals so colorful? What are the adaptive and perceptual meanings of polychromatism?

To answer these questions, flower and bird colorations were studied psychophysically.

On the basis of the experimental results, the answer to the question “what is the visual purpose of color?” is tripartite as follows. (i) To relate each chromatic component of an object, thus favoring the emergence of the whole object. (ii) To show a part-whole organization where both components are not weakened but reciprocally enhanced one by virtue of the other and within the whole. (iii) To show fragments to hide the whole and favor the emergence of single components. In summary, color influences wholeness, part-whole organization and phenomenal fragmentation. Finally, a new kind of camouflage, “Harlequin camouflage”, is proposed.

How can a fish hide in the open ocean?

Robert Greenler
Madison, Wisconsin

Abstract

Under certain lighting conditions, a fish, whose scales have appropriate reflective properties could, in principle, be invisible in open water. Studies have shown that some fish have developed such camouflage capabilities.

Iridescent colors in spider webs

H Joachim Schlichting

Institut für Didaktik der Physik, University of Muenster, 48149 Muenster, Germany (Schlichting@uni-muenster.de)

Spider orb webs which normally appear grey sparkle in vivid colors if they are viewed at grazing incidence with regard to the sun. Although it is well known that the origin of these colors is the diffraction of the sunlight, “a full explanation … has not yet been given …” according to Livingston [1]. We try to complete former investigations [2] by studying effects due to almost regularly spaced droplets on the capture thread of an orb web [3]. This is done in experiments as well as theoretical considerations.

From an optical point of view droplets on a thread represent a periodic linear array of scattering elements acting as a kind of diffraction grating. We will show that this grating is of great importance for the understanding of the overall scattering pattern. The structure elements of this pattern can be assigned to three different sources of diffraction:

- the thread of the web,
- the nearly identical segments consisting of a droplet and the section of the threat between two drops and the droplets.

The experimental findings are described and compared with results of a simplified model.

References

[1] Livingston B: Glorious visions: colour and light in nature *J. Br. Astron. Assoc.* **115 (2005)** 247–9
[2] Greenler R G and Hable J W: Colors in spider webs *Am. Sci.* **77 (**1989) 369–73
[3] Suhr, W and Schlichting, H J: On the Colours of spider orbs webs *Eur. J. Phys.* **32** (2011) 615–624

Structural color of the butterfly wing scale

S. Yoshioka, Osaka University

The color pattern of the butterfly wing consists of the arrangements of differently colored wing scales: each scale has generally one color, and the arrangement of scales with different colors produces the wing color pattern as a mosaic. The attached figure clearly shows a diversity of color and shape (typical length of a scale is 100 μm). These scales were collected from the wings of about ten butterfly species. Some of them contain pigments that absorb light in some wavelength range, while others have sculpted microstructures on their surfaces in a size that is comparable with the wavelength of light. Such structures cause optical interference and may result in iridescence and also highly-efficient wavelength-selective reflection. Thus, the butterfly wing scales are abundant in optical phenomena.

In this paper, we will review the structural colors of the wing scales of some species of butterflies. Optical phenomena caused by various types of microstructures are treated. It is also emphasized that not only microstructures, but large-size structures, pigments, and overlapping of several scales can also contribute to the beautiful coloration of the butterfly wing.

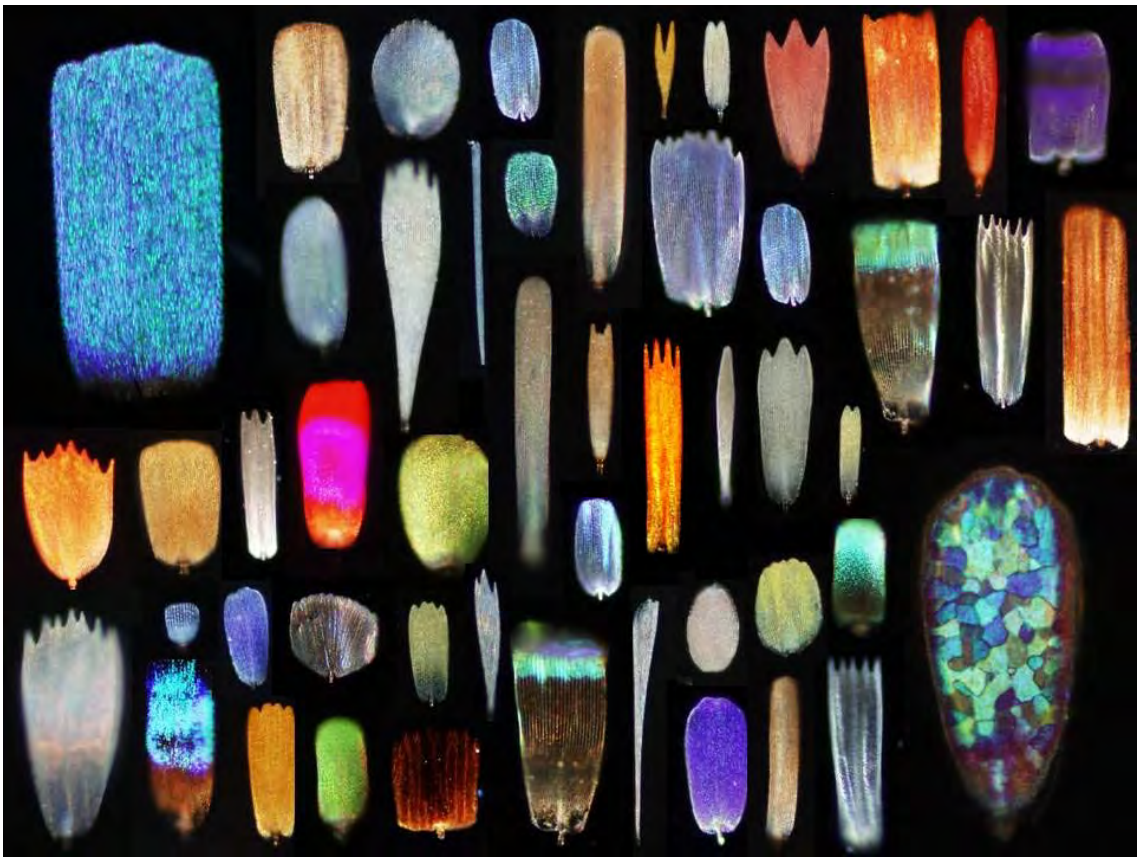

Total internal reflection as solar protection for the Saharan desert ant Cataglyphis bombycina

Priscilla Simonis and Jean Pol Vigneron

Research Center in Physics of Matter and Radiation (PMR), University of Namur,
rue de Bruxelles, 61, B-5000 Namur Belgium

The desert ant Cataglyphis bombycina (Formicidae) is one of the terrestrial living organism best prepared to stand high temperatures. One of the most obvious features is its white metallic color, which protects the ant's body from the solar radiation. The high optical reflection is obtained on a dense covering of the body by bristles which assume a triangular prismatic shape. The tiny prisms are oriented with a flat basal plane parallel to the cuticle surface and it is shown that total reflection conditions are satisfied on this face for light entering and exiting through the other faces. The entry and exit faces are configured to maximize light transmission by a diffractionless corrugation.

Visible and invisible mirages:

Comparing inferior mirages in the visible and thermal infrared spectral range

Michael Vollmer, Brandenburg University of Applied Sciences, Germany, vollmer@fh-brandenburg.de
Joseph A. Shaw, Paul W. Nugent, MSU Bozeman, USA

Abstract:
Visible light and thermal infrared inferior mirages in the wavelength range from 7 to 14 µm have been observed and recorded simultaneously for take off and landing of various airplanes on the runway of Bozeman airport /Montana for distances of a few km (Figs. 1,2). In addition IR mirages were also recorded for cars on a hot summer street and distances below 1 km. There are many similarities between the VIS and IR mirages. However, infrared mirages show also some interesting differences which relate to the involved physics such as transient heating effects of the tires upon landing.

Fig. 1: Snapshots from an IR video, showing mirages observed in thermal infrared for a plane during landing. In addition, the sequence of touching of the tires is clearly visible.

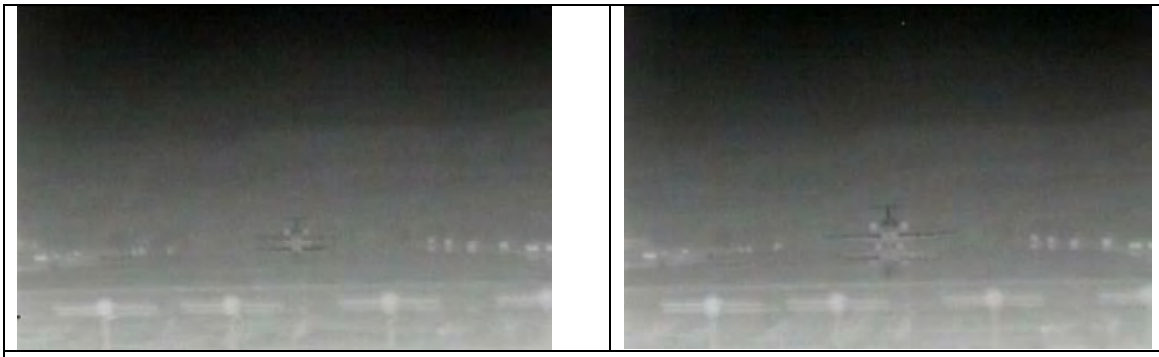

Fig. 2: Examples for mirages observed during take off.

(Invited talk)

The natural tertiary rainbow – a photographic first

Michael Grossmann, AK Meteoros, Kaempfelbach, Germany

The author took an early interest in natural photography, and later then was attracted to atmospheric optics. With the coming of the digital age in photography he started hunting for halos, sunset and twilight phenomena and rainbows, mostly from a 1000 ft hill with a 360 deg unobstructed horizon near his village in southern Germany. Making friends with other enthusiasts helped sharpen his eye for even rarer phenomena in the sky. First basement experiments with water droplets and laser light quickly showed many rainbow orders. After being briefed on the then disputed visibility prospects of a natural tertiary rainbow from the 10th Light & Color in Nature Conference, he set out to look for it on any feasible occasion, especially in heavy rain and storm. In the spring of 2011, an odd false alarm came with a circular glare caused by a droplet on his camera lens. Then, on May 15th, 2011, the bow was caught. In his talk the author will put an emphasis on the excitement and aftermath of his breakthrough observation, which up to now has only been matched and superseded once, and also tell of future projects.

Abstract submitted to

Light and Color in Nature
August 5-8, 2013
Fairbanks, AK, USA

Title

Photographic observation of a natural fifth-order rainbow

Author

Harald E. Edens

Abstract

A photograph has been obtained of a primary and secondary rainbow that shows evidence of a fifth-order (quinary) rainbow. The photograph was taken in the evening of August 8, 2012 at the Langmuir Laboratory for Atmospheric Research, located at 3.2 km altitude in the Magdalena Mountains of New Mexico, USA. The camera was a Nikon D700 digital camera fitted with a 24-70 mm f/2.8 lens set at a focal length of 68 mm and f/8. A circular polarizer was used, adjusted to maximize contrast of the rainbows with the background. Although the unprocessed image does not show clear evidence of the fifth-order bow apart from hints of a green band, a contrast-enhanced image shows a broad, green band bordered on the inside by a blue-violet band.

The orientation of the photograph was calibrated using the coordinates of landmarks. RGB color values were read from the photograph as a function of scattering angle, and compared with numerical Debye-series simulations. The fifth-order bow appears in the location predicted by simulations. The simulations were matched to the spacing of supernumeraries to the primary and secondary bows, indicating that the bows were produced predominantly by 0.6 mm diameter droplets.

Polarization and visibility of higher order rainbows

Gunther Können

The degree of polarization of rainbows of order k with $k \geq 3$ is bounded in the interval [75%, 80%], where 75% is the limit for $k \to \infty$. A polarizer can improve the signal to background ratio of the 3rd and 4th rainbow by a factor 2, which may lift their visibilities in natural circumstances above the threshold of human visual perception. The prospect for observing the 5th or 6th rainbow in Nature are unclear. There exist a slight possibility that the signal of the natural 7th rainbow (appearing at 64° from the Sun) may be separated from its background if photographed under perfect conditions through a polarizer.

Recent Rainbow Revelations

Robert Greenler
Madison, Wisconsin

Abstract

This presentation is a sketchy history of our understanding of rainbows, with emphasis on recent searches for higher-order rainbows in the visible, infrared, and ultraviolet spectral regions.

New insights into the rainbow

Jean Louis Ricard[1,2], Peter Adams[2] and Jean Barckicke[2,3]

1 = CNRM, Météo-France,42 Avenue Gaspard Coriolis, 31057 Toulouse, France
2 = CEPAL, 148 Himley Road, Dudley, West Midlands DY1 2QH United Kingdom
3 = DPrévi/Compas,Météo-France,42 Avenue Gaspard Coriolis, 31057 Toulouse, France
Dr_Jean_Ricard@yahoo.co.uk

Part 1: Impact of the solar height upon the natural rainbows

A realistic model of the rainbow has been developed. It is based on the Airy theory. The main entry parameters are the droplet size distribution, the angle of the sun above horizon and the temperature of the droplets and the wavelength. It is usually assumed that the overall aspect of the rainbow is mostly dependant on the size of the droplets, but our results show that it is usually NOT the case. The most important parameter for natural rainbows is usually the height of the sun above the horizon.

Part 2: Study on the physics of the supernumerary bows

Jean Louis Ricard[1,2] and Peter Adams[2]

1 = CNRM, Météo-France,42 Avenue Gaspard Coriolis, 31057 Toulouse, France
2 = CEPAL, 148 Himley Road, Dudley, West Midlands DY1 2QH United Kingdom

We have tested the basic assumptions of the Airy's theory. Surprisingly, they are only valid in a small angle close to the minimum deviation angle (less than 2 degrees). For instance in the supernumerary area, the Airy's theory has obvious flaws. In the Airy's model, two aspects of the diffraction are taken into account. Firstly, a phenomenon of interferences discovered by Young created by rays of light with different pathes through the droplets. Secondly, "simple diffraction" such as the one appearing on the both (shadowed and lighted) side of a straight edge. In this study, we show that the "simple diffraction" alone is enough for understanding the formation of the supernumerary arcs. Interferences contribute in fact only very little.

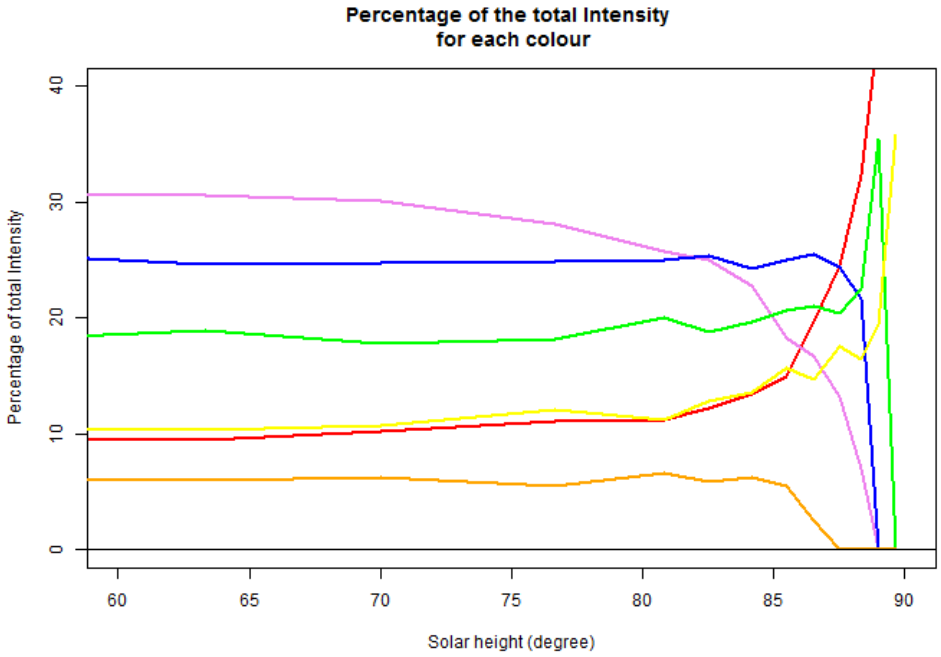
Percentage of the total Intensity
for each colour
Percentage of total Intensity
0
10
20
30
40
60
65
70
75
80
85
90
Solar height (degree)

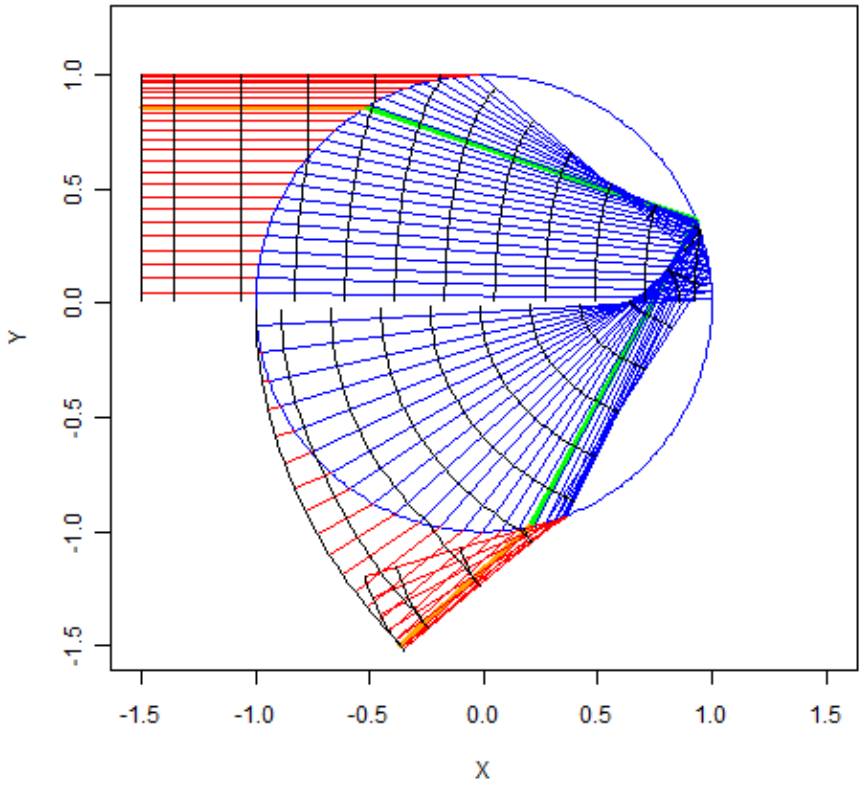
Y
1.0
0.5
0.0
-0.5
-1.0
-1.5
-1.5
-1.0
-0.5
0.0
0.5
1.0
1.5
X

Observation, photogrammetry, and analysis of a twinned rainbow

Alexander Haußmann, Pfotenhauerstraße 32, D-01307 Dresden, haussmann@iapp.de

On May 11th 2012, a bright and well-developed twinned rainbow was visible after the passing of a mild thunderstorm in Dresden, Germany. Due to a well defined observation position, it was possible to precisely locate the celestial position of the rainbow by calibrating the photographs with the help of a starfield image taken some time later. The resulting intensity characteristics for different clock angles allow the reconstruction of the effective drop size distributions along the rainbow cone, i.e. the average over multiple showers and illumination conditions along the line of sight. To do so, a rainbow model based on realistic drop shapes is required, e.g. as presented in [1]. However, since simulation software relying on this comprehensive approach is not available yet, a simpler model based on Airy theory and a drop shape description as conjoined half-spheroids with different oblatenesses is used for the purpose of this work. The results indicate that twinned (or even ordinary) rainbows might prove to be useful as remote sensing tools for the optical determination of rainfall properties.

[1] I. Sadeghi et al., *ACM Transactions on Graphics* **31**, 3 (2012).

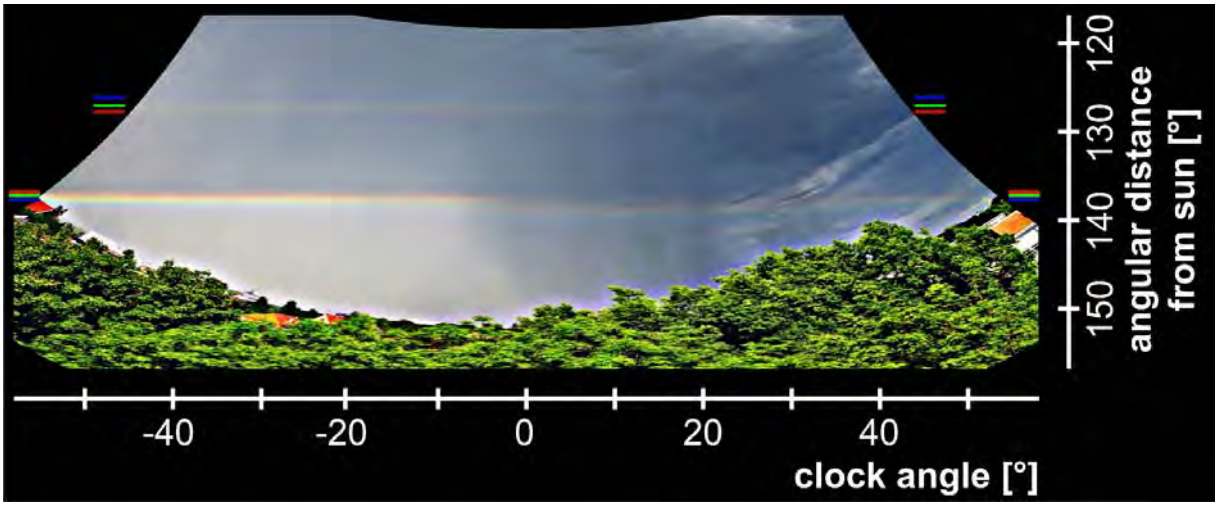

A PHYSICALLY-BASED RAINBOW SIMULATOR TAKING THE BACKGROUND INTO CONSIDERATION

MOON R. JUNG

Abstract. Recently we implemented a system for spraying and lifting waterdrops to create large-scale rainbows, as shown in Fig. 1 and 2. To better understand the process of rainbow generation, we develop a simulator which generates images of rainbow based on atmospheric optical laws. To produce photo-realistic images, we have taken efforts to combine the research and developments conducted by both fields: computer graphics and atmospheric optics. From the computer graphics, we took the software framework, called Mitsuba, for implementing a generic radiative transfer equation and generating images. To this framework, we add a plug-in program that provides the necessary parameters to the radiative transfer equation: the scattering coefficient, and absorption coefficient, and phase function for the waterdrop medium. Using Mitsuba we produce the intensity of light arriving at the eye of the viewer for each of a discrete number of wavelengths (e.g., 30) in the visible spectrum 360-830 nm. Then we generate a RGB image from the spectral images for each wavelength. The scattering coefficient of waterdrop medium, which is defined to be the scattering cross-section of waterdrops per unit volume, is computed from two given parameters: the number density of waterdrop medium, and the scattering cross-section of a waterdrop. In this paper, the scattering cross-section of a waterdrop is computed by means of ray-tracing based on geometric optics. Geometric optics does not consider the interference among rays that the same wave produces as it passes through the same drop. But we use geometric optics assuming that waterdrops have a statistical distribution of sizes, and thus the mentioned interferences of waterdrops cancel each other to a considerable extent. The absorption coefficient and phase function of waterdrop medium are also computed by ray tracing. Also, the influence of the background is incorporated into rainbow simulation. First, we study how the perception of rainbow is influenced by the brightness contrast between the rainbow and the background including clouds, terrain, mountains, and buildings. Second, we study how the perceptions of rainbows size and distance are influenced by the background, especially terrain and buildings.

Dept of Art Technology, Graduate School of Creative Media, Sogang University, Seoul, Korea

E-mail address: moon@sogang.ac.kr

FIGURE 1. A rainbow created by our system. Its length looks like 70 100 m for human eyes.

FIGURE 2. A rainbow viewed from another angle.

Influence of non-spherical raindrop shapes on higher order rainbows

Alexander Haußmann, Pfotenhauerstraße 32, D-01307 Dresden, haussmann@iapp.de

Deviations from the spherical shape of raindrops are known to significantly influence the resulting primary and secondary rainbows. Recently, a comprehensive theoretical model involving realistic drop shapes has been proposed to account for these effects with an accuracy on the level of the Lorenz-Mie theory [1]. Moreover, a possible amplification effect for the third order rainbow due to drop oblateness was already discussed at the 10th L&C conference in June 2010 [2]. In this contribution, the results of geometrical optics raytracing for asymmetrically flattened drops (represented as conjoined half-spheroids with different oblatenesses) and realistic drop size distributions for rainbows up to the 5th order will be discussed. Though geometrical optics cannot address finer features like supernumerary arcs or diffraction catastrophes, more general trends such intensity increases at certain parts of the bows' circumference are likely to be represented correctly, hence providing suggestions where to look at to find natural higher order rainbows.

[1] I. Sadeghi et al., *ACM Transactions on Graphics* **31**, 3 (2012).

[2] R. L. Lee, Jr. and P. Laven, *Applied Optics* **50**, F152 (2011).

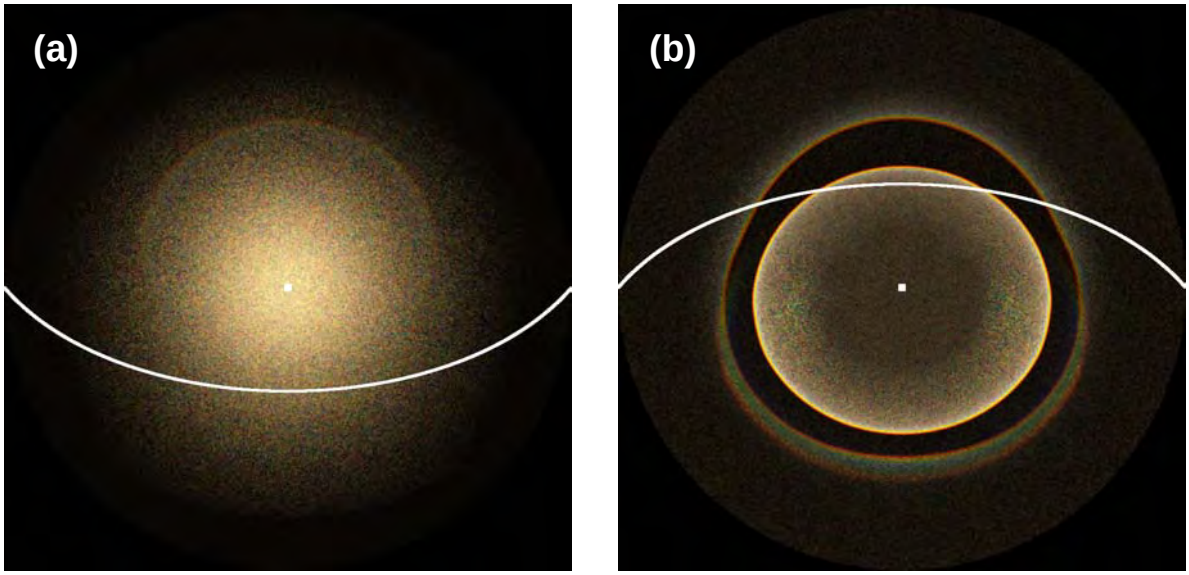

Intensity distributions at 30° solar elevation for raindrops of 0.75 mm effective radius. (a) forward direction, showing conjoined 3rd and 4th order rainbows embedded in the zero order glow, (b) backward direction, showing distorted primary and secondary order rainbows and the 5th order rainbow beneath the secondary.

Flashes of light below the dripping faucet: an optical signal from capillary oscillations of water drops.

T. Timusk

Department of Physics and Astronomy, McMaster University

The Canadian Institute of Advanced Research

Abstract

Falling water drops from a dripping faucet, illuminated from above, exhibit a row of bright strips of light, a few centimeters apart at a fixed distance below the faucet. High speed photography of the drops shows that they are oblate in shape when the flashes occur. The flashes originate from the edge of the drop on the opposite of the overhead light source *i.e.* the same path trough the drop that gives rise to the rainbow in spherical drops. The periodic flashes reflect the capillary oscillations of the liquid drop between alternating prolate and oblate shapes and the dramatic enhancement in the oblate phase result from a combination of several optical effects. Ray tracing analysis shows[1] that the flashes occur because the rainbow angle (42° in spherical drops) sweeps over a wide range between 35° and 65° for typical oscillating ellipsoidal drops and the intensity of the caustic is strongly enhanced in the oblate phase. This phenomenon is ubiquitous and can be seen in all brightly lit water sprays with millimeter size drops and is responsible for their white color.

[1] T. Timusk, Applied Optics **48**, 1212 (2009).

(Invited forum)

A Post-Faustian Review of Digital Imagery: the Good, the Bad and the Weird

Introduction to the Digital Imagery Discussion Session

David K. Lynch
Thule Scientific

Abstract

Driven by faster computers, hard-coded digital image operations in cameras, vast digital storage space and millions of users inventing new ways to acquire and manipulate digital pictures, digital imagery has become both ubiquitous and diverse. But as indicated by the fact that many camera manuals weigh more than the camera, a lot more understanding must be acquired to fully exploit the images without misrepresenting them. As Ken Sassen said a few months ago, “It comes down to honest reporting.” But is that even possible? Six people with six different cameras taking pictures of the same scene will take six measurably different pictures.

When many of us take a nice shot, the first thing we do is click the “Adjust Image” icon and start tweaking. The resulting instant gratification is often accompanied by a sense of guilt, because (1) we’re modifying the sacred original, and (2) we usually don’t know what the “Adjust Image” button really does. But, it makes the picture somehow better, at least by our subjective standards. Bad enough (or is that good enough?) that the jpeg output has a gamma curve applied to it (even some raw formats do), but it is essentially a logarithmic retelling of the image. Some cameras come with a built-in capability to do High Dynamic Range imagery (HDR), a magical black box that produces wonderfully revealing, if not somewhat painted-looking, images.

As scientists interested in visual phenomena, we may find ourselves pulled between two legitimate but opposing forces: radiometric accuracy versus the desire to show photographs that portray what we saw with our eyes, not what the camera recorded. Since the eye and a digital sensor record light in profoundly different ways, a digital image is a far cry from a straight brightness map of the scene presented to the eye (the same was true of film, but in uglier though more comprehensible ways).

Yet even before digital cameras, we were doing tricks to get clever pictures that simply could not be seen with the naked eye: time exposures, panoramas, using polarizing and skylight filters, high speed shutters, etc. Digital imagery didn’t invent these tools, only enhanced and spread them. But digital cameras and image manipulation software are here to stay because they offer so much more versatility than film cameras ever could.

In this opening talk, I will discuss a few aspects of digital imagery, starting with radiometric accuracy. After a few more comments, I will open the floor to discussion.

Seeing, Adapting to, and Reproducing the Appearance of Nature

Mark D. Fairchild
Rochester Institute of Technology
Associate Dean of Research & Graduate Education, College of Science
Professor of Color & Imaging Sciences
mdf@cis.rit.edu

Abstract

The perception of color in nature is a complex multi-dimensional phenomenon. The vast range and high dimensionality of the light stimulus in a natural scene are reduced by the human visual system. The color experience is reduced to the appearance attributes of brightness, lightness, colorfulness, saturation, chroma, and hue from the spectral energy distributions in the scene while the vast range of light levels present in nature is reduced to a more manageable perceptual range through local adaptation and response compression. These processes set the stage for efforts to capture, process, and reproduce the colors of nature as well as make artistic interpretations of them. This paper discusses the challenges involved in measuring light phenomena in nature, modeling the human perception of these phenomena, and then attempting to reproduce the visual appearance of nature using necessarily-limited image display technology. The techniques and data of quantitative high-dynamic-range imaging to capture scene information, color and image appearance modeling to predict human visual response to the scene, and color and tone mapping to characterized image displays to reproduce the appearance of the scene are reviewed to describe a coherent theory and process on appearance reproduction of natural visual phenomena.

Figure 1. A simplification of the colors in the General Grant Tree image (from Kings Canyon NP, http://www.cis.rit.edu/fairchild/HDRPS/Scenes/GeneralGrant.html). The left panel shows each of the nine captured exposures reduced to 100 colors by spatial sampling. The middle panel shows the HDR image (constructed from the 9 exposures) sampled down to 100 colors and the right panel shows a visual rendering through local adaptation also sampled down to 100 colors. All are valid samplings of the colors in the scene, but only the right panel is a reasonable representation of the colors an observer would perceive when present in the original scene (even though the center panel is a closer physical reproduction of the scene colorimetry). The coarse sampling allows visualization of the scene colors without the confound of the specific image content. For comparison, full resolution images and the processes used to reproduce accurate color information will be presented in the talk.

What is the spectrum of skylight polarization?

Joseph A. Shaw and Nathan J. Pust, Montana State University, Bozeman, Montana, USA (jshaw@montana.edu)

Abstract

There seems to be interest and confusion regarding the question of how skylight polarization varies with wavelength. It is commonly known that optical scattering by atmospheric gas molecules gives rise to significantly polarized skylight, but it is less commonly known that scattering by aerosols, clouds, and the underlying surface very strongly reduce the skylight degree of polarization. Because these competing effects all vary with wavelength, the spectrum of skylight polarization can vary widely depending on what kind of aerosols, clouds, or surface reflection properties exist at any given location at any given time. Human observers still see the expected polarization enhancement that reaches a maximum 90° from the sun, but without careful measurements they may not realize how very different the polarization spectrum can be from time to time. We use polarized skylight simulations initialized with actual measurements of aerosols and surface reflectivity to illustrate how widely variable the skylight polarization spectrum can be. The model we use has been validated carefully through comparison with sky-polarization images acquired with our all-sky polarization imager.

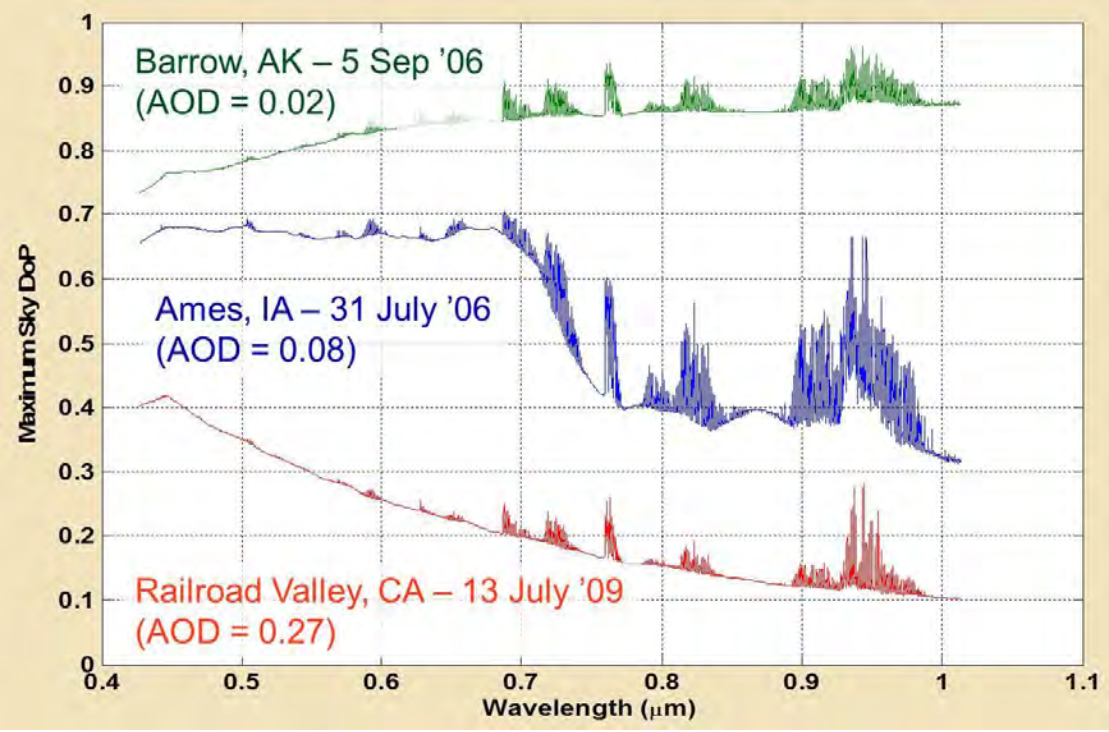

Figure 1. Three widely varying examples of skylight polarization spectra that are explainable through a combination of aerosol and surface properties.

Raymond Lee, United States Naval Academy (raylee@usna.edu), "Measuring haze's effects on the colors and visible-wavelength spectra of clear skies"
submitted to 2013 Light and Color in Nature conference at the University of Alaska—Fairbanks

Abstract: To casual observers, haze's visible effects on clear daytime skies may seem mundane: significant scattering by tropospheric aerosols distinctly (1) reduces the contrast of distant objects and (2) desaturates sky blueness. Depending on haze droplets' constituents (*e.g.*, dissolved sulfates or sea salts, insoluble soot or mineral inclusions, various anthropogenic pollutants), multiple scattering by haze may or may not visibly alter clear-sky hues. At the U. S. Naval Academy (USNA) in Annapolis, Maryland, we usually experience hazes that are dominated by dissolved sulfates and sea salts, which by themselves cause no immediately apparent hue (as opposed to saturation) shifts in skylight.

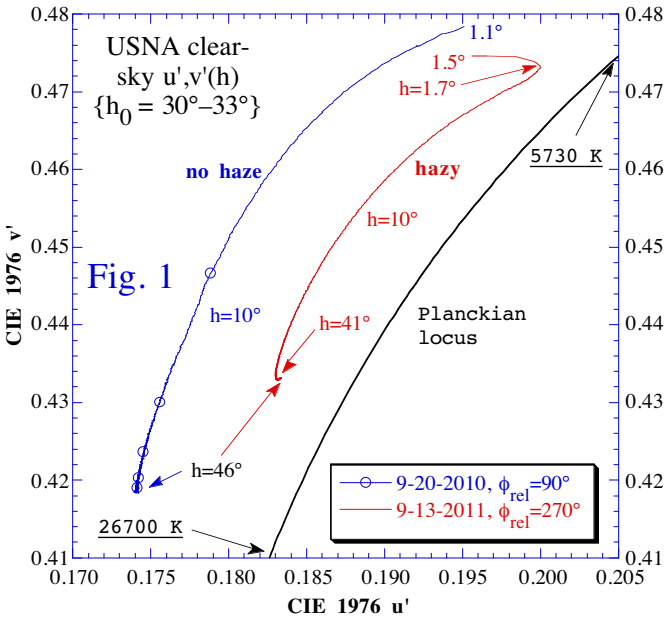

However, colorimetric and spectral measurements made at USNA with both multispectral and hyperspectral imaging systems consistently reveal *visible* spectral shifts in hazy skylight.

For example, Fig. 1 shows part of the CIE 1976 uniform-chromaticity-scale (UCS) diagram, including the Planckian locus for a range of color temperatures. To the left of this locus are two skylight chromaticity curves calculated from hyperspectral scans made along sky meridians (*i.e.*, from low to high view-elevation angle h at a constant azimuth relative to the sun ϕ_{rel}). One scan is from a hazy day (9-13-2011; 500-nm aerosol optical depth $\tau_{aer} \sim 0.227$) and the other is from a visibly haze-free day (9-20-2010; 500-nm $\tau_{aer} \sim 0.0372$). Because the unrefracted sun elevation $h_0 \sim 30°$ for each scan, they cover the same range of single-scattering angles along their respective sky meridians.

Yet the two skies' chromaticities differ both graphically and visually: compared with its haze-free counterpart, the hazy-sky curve (a) has a much smaller colorimetric gamut, (b) is closer to the Planckian locus' near-neutral colors, and (c) has distinct chromaticity "hooks" at low and high h. Although features (a) and (b) roughly correspond to visual observation (2) above, feature (c) is unexpected, as is the greenward shift (*i.e.*, toward the upper left) of the entire haze-free curve. Because most such changes in haze-dependent colors greatly exceed local MacAdam just-noticeable differences, with practice one can actually *see* them on different days. However, consistently producing these color changes in radiative transfer models such as MODTRAN is more problematic. I plan to discuss these and other spectral consequences of tropospheric haze in my proposed talk.

Views affected by a wavy air-water surface

Yoav Y. Schechner

Dept. Electrical Engineering

Technion – Israel Inst. Technology

Haifa, Israel 32000

www.ee.technion.ac.il/~yoav

yoav@ee.technion.ac.il

Scenes affected by a wavy water-air interface (WAI) are common and have natural and engineering importance. Marine animals (archer fish, birds) view through a WAI to detect and aim at prey beyond the WAI. Some animals may take this difficult view to detect and avoid predators beyond the WAI. For humans, this view is imposed in remote sensing of the ocean, and can also form a *virtual perisocope*, where airborne scene are observed by a submerged diver, without an attention-drawing probe. In all cases, the wavy WAI creates distortions that are random in space and time, significantly complicating vision. Nevertheless, using statistics of WAI waves, statistics of random refractive distortions are derived per view angle. This enables us to derive stochastic localization and triangulation of objects, and discrimination of moving objects, despite overwhelming dynamic distortions.

The WAI plays a role also when it is not on the line of sight. A wavy WAI creates caustic networks: random spatiotemporal illumination patterns. They strongly affect shallow underwater scenes. However, these random natural patterns encode the three-dimensional underwater structure. We thus show how this 3D structure can be retrieved very simply and accurately. Furthermore, the retrieved structure enables estimation and inversion of water scattering effects, particularly when the viewer moves in this complex scene.

Simulating Dark Sunlit Clouds

Stanley David Gedzelman

David Lynch

Abstract

Optically thin sunlit clouds tend to appear dark in the part of the sky near the antisolar point. A simple, analytic theory that explains this observation in terms of the large asymmetry parameter of the angular scattering phase function of cloud droplets is revisited.

The lighting and color of sunlit clouds are then simulated using a multiple scattering, Monte Carlo beam tracing model. Sunbeams undergo Rayleigh scattering by air molecules or Lorentz-Mie scattering by tiny aerosol particles in clear air and Lorentz-Mie scattering by droplets in individual clouds. Several cloud shapes are used including boxes, top slices of a sphere, or oblate spheroids of various eccentricities. Optical thickness and droplet spectra characteristic of cumulus and lenticular altocumulus are free parameters of the model. Dot maps that show the angular scattering distribution of light emerging from all sides of the clouds are given. Simulated images of the sky and clouds with near photographic quality are produced by filing the dots in bins of small angular width that cover the visual field and then smoothing and normalizing the light intensity at 61 wavelengths for the field of bins.

Shadows

David K. Lynch

Thule Scientific

Abstract

We investigate the brightness distribution of umbral shadows for a variety of sky conditions (primarily clear and overcast) and atmospheric scattering parameters using geometrical optics. Small shadows have a nearly uniform brightness distribution while large shadows are much darker at their centers. The presence of an occulter (e.g. cloud) in the sky influences the brightness of sunlit portions of the ground because it blocks part of the sky radiance. The aureole has a significant influence on the brightness of the edge of shadows, as do the bright edges of isolated clouds. The approach used to analyze shadows also applies to the brightness inside caves and wells.

Raymond Lee, United States Naval Academy (raylee@usna.edu), “Twilight’s Belt of Venus: Mythology, Measurements, and Modeling”

submitted as invited-paper candidate to 2013 Light and Color in Nature conference at the University of Alaska—Fairbanks

Abstract: Near the antisolar horizon during clear twilights, the rose-colored band of the antitwilight arch often appears, adjoined by the bluish-gray wedge of the dark segment (or earth’s shadow) beneath it. Although the antitwilight arch is a commonplace of civil twilight, sometimes it goes by a far more exotic name — the belt of Venus.

What are this remarkable synonym’s origins? Might they include some characteristic visible and spectral features of the belt of Venus? Because the planet Venus is seen during twilight only near the *solar* horizon, at first glance the antitwilight arch may seem unconnected to it.

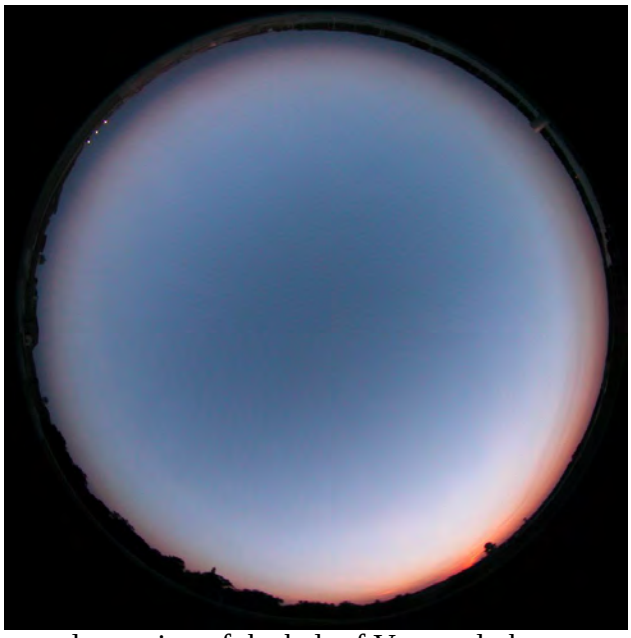

Yet fisheye images of clear twilights show that our present-day tidy partitioning of the horizon sky (and the associated naming of its parts) may partly explain this disconnect. A more surprising link to Venus comes from Greco-Roman mythology, in which the literal belt or girdle of Venus was a highly prized divine adornment that aroused irresistible ardor for anyone who wore it. Strangely, the term became a medieval and Renaissance euphemism for a chastity belt.

Until recently, detailed colorimetric and spectral mapping of the belt of Venus, dark segment, and other twilight features has been problematic because sky luminances change so rapidly then. My research using multispectral and hyperspectral imagers, including ordinary RGB digital still cameras, solves such problems and reveals some characteristic color signatures of these features. The difficult challenge for radiative transfer models such as LOWTRAN7 is to consistently reproduce these features’ unusual color gamuts.

Visibility of Sirius in broad daylight

Gunther Können and Piet Stammes

Royal Netherlands Meteorological Institute, de Bilt, The Netherlands

In 1988, we spotted Sirius with the naked eye at broad daylight by looking along the finder of a 1-m telescope on La Palma Observatory, at 2400 m height. Sun elevation was 73°; Sirius was straight under the sun at 37° elevation. The sky radiance, although not recorded directly, could be estimated from the simultaneously obtained wavelength-depended sky polarization data near Sirius. This was done with the Doubling-Adding KNMI (DAK) radiative transfer model, a model suited to calculate multiple scattering of polarized light in the Earth's atmosphere. From the optimal fit with the observed polarization provided values of the surface albedo the aerosol optical thickness, from which the sky radiance at any altitude could be calculated. A daylight zenith limiting magnitude at sea level of -1.2 or better for sun elevations up to 50°. This implies that Sirius (magnitude -1.46), when positioned overhead, can be a naked eye object even if its culmination occurs at noon.

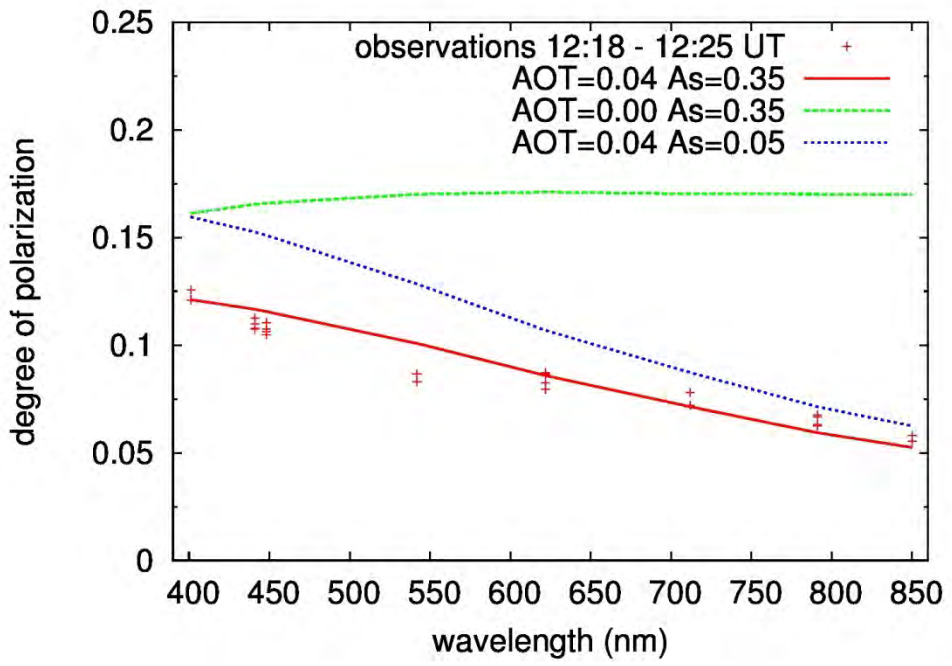

Figure 1: Sky polarization near Sirius obtained instrumentally during the visual observation. Crosses: observed degrees of polarization. Solid line: Calculated polarization for aerosol optical thickness (AOT) 0.04 and surface albedo (As) 0.35. The dashed curves demonstrates that AOT and As are both needed for obtaining a good fit to the observations.

Some Elementary but Surprising Facts about the Sun's Location in the Sky

A. James Mallmann and Steven P. Mayer, Milwaukee School of Engineering, Milwaukee, WI

Over the recent decades investigations and studies of the interactions of rays of sunlight with raindrops and with airborne ice crystals have resulted in a better understanding of rainbows, halos, sun dogs, sun pillars, and of many other patterns of light and color in the sky. I will report on some simpler observations about where the Sun is in the sky and the Sun's path in the sky. Consideration of some of those observations inspired calculations and measurements that surprised me, and may surprise you as well.

Earthshine Brightness and Visibility

David K. Lynch
Thule Scientific

Abstract

Earthshine is sunlight reflected from the Earth to the dark side of the Moon, then back again to observer on Earth. Its origin was first explained by Leonardo da Vinci[1] in the Codex Leicester between 1506 and 1510. Earthshine has found a number of uses including monitoring global cloud cover, and searching for extraterrestrial planets and life ("planetshine"). It is also well represented in literature, art and folklore.

Lunar crescents go hand-in-hand with earthshine. Both being faint and seen in twilight, many of the same factors that influence crescent visibility also affect earthshine visibility. While much has been written about crescent visibility because of its religious importance - relatively little work has been done on earthshine visibility. In this paper we set forth a simple model of the earthshine's brightness and discuss its naked eye visibility.

The Use of Light and Color in Astrophysical Imaging

Travis A. Rector (University of Alaska Anchorage), Zoltan Levay and Lisa Frattare (Space Telescope Science Institute), Jayanne English (University of Manitoba) and Kirk Pu-uohau-Pummill (Gemini Observatory)

Astronomers frequently use telescopic data to create "color composite" images, for use in scientific visualization as well as for public outreach. Telescopes not only magnify an object, they also amplify faint light as well as detect kinds of light outside of the optical window. It is no exaggeration to say that telescopes can see the invisible, at least as defined by human vision. So how then do we translate what the telescopes can see into a color image that we can see? The methodology is not unambiguous, but it is also not without guiding principles. As part of this talk, how color composite images are created for several professional observatories, including Kitt Peak National Observatory, Gemini Observatory and the Hubble Space Telescope, will be described. The discussion will include how data from many different wavebands can be combined to produce a color image, as well as how colors are chosen to do so. Several examples will be given. The talk will also describe the expectations of scientists and the public, and how they can be different.

Lunar Eclipse Photometry Across the World – First Correlations

Elmar Schmidt, SRH University of Applied Sciences, Heidelberg, Germany

After reporting a measuring method capable to yield absolute visual magnitudes for the total lunar eclipse (TLE) of March 3rd, 2007 in the 9th Light & Color in Nature Conference, the author traveled to premier astronomical sites for all five other TLEs since then. For three out of these a complete light curve was obtained (the two other tries failed because of bad weather). Although all data were taken from high altitude sites, they were corrected to unit air mass at sea level. At first, a consistent record of the strong lunar opposition surge arose in terms of absolute luminance. The intensity and color of the Moon during totality is known to be sensitive to the state of the Earth's high atmosphere, especially its aerosol and ozone content. Plotting the data for several eclipses over their umbral (=geometrical) magnitudes shows a good correlation, disproving global anomalies of the high atmosphere, at least for these events.

Using light and color to detect life on Earth-like extra-solar planets

Eyal Schwartz, Stephen G. Lipson and Erez N. Ribak
Physics department, Technion – Israel Institute of Technology, Haifa 32000, Israel

Abstract

Detecting extra-solar planets is considered by far one of the most challenging fields in observational astronomy. In particular, the discovery of an Earth-like extra-solar planet (exoplanet) which shows signs of life would be an incredible achievement. We are aware that evolution of life there might be completely different from that on Earth; however, it would require some form of photosynthesis based on complex molecular chemistry which would be indicated in the observed bio-signatures. The main observational problem is the very faint light signal of such an exoplanet close to an overwhelmingly bright parent star. We have proposed a method [1] which exploits Fourier interferometric spectroscopy in the mid-IR, where planet-star contrast is most favorable, to maximize the relevant information obtained during a limited telescope exposure time. The method concentrates on typical features such as band widths which are dictated by the complex structure, without being restricted to a specific type of chemistry, and can improve the spectral planet-to-star signal ratio by many orders of magnitude. New laboratory experiments indicate the feasibility of this approach, which can be implemented on existing interferometric telescopes such as Very Large Telescope Interferometer (VLTI) in Chile.

[1] Schwartz E. et al., 2012, Astronomical Journal, **144**, 71